

TOHOKU UNIVERSITY



DOCTORAL THESIS

**Estimation of soil salinity and its effects
on rice yield in Banphai, Northeast
Thailand**

Author:

YANG YI

Supervisor:

Professor Koki Homma

*A thesis submitted in fulfillment of the requirements
for the Doctor of Philosophy*

of the

Crop Science

Faculty of Agriculture

Graduate School of Agriculture

August 23, 2023

Declaration of Authorship

I, YANG YI, declare that this thesis titled, "Estimation of soil salinity and its effects on rice yield in Banphai, Northeast Thailand" and the work presented in it are my own. I confirm that:

- This work was done wholly or mainly while in candidature for a research degree at this University.
- Where any part of this thesis has previously been submitted for a degree or any other qualification at this University or any other institution, this has been clearly stated.
- Where I have consulted the published work of others, this is always clearly attributed.
- Where I have quoted from the work of others, the source is always given. With the exception of such quotations, this thesis is entirely my own work.
- I have acknowledged all main sources of help.
- Where the thesis is based on work done by myself jointly with others, I have made clear exactly what was done by others and what I have contributed myself.

Signed:

Date:

Acknowledgements

I would like to express my deep appreciation to all those who have provided me with encouragement and support in the past 3 years as at the beginning of thesis.

First and foremost, I sincerely thanks to my supervisor, professor Homma, who has provided a lost guidance, suggestions, and encouragements both in my life and study. His profound insights and novel viewpoints have greatly contributed to my personal and scholarly growth throughout my academic journey., without his precious comments, the thesis would not be what it is now.

Secondly, I would like to express my deepest thanks to my adoring spouse, Mr. Feng. I am truly thankful for his unwavering support and companionship throughout my academic journey, from my master's degree to my PhD. It is undeniable that without his love, I would not have become the person I am today.

Thirdly, my thanks also go to the assistant Nakajima and all student in crop science laboratory. Especially, my senior doctor Ye. They have provided me a lot of supports both in life and study.

In addition, I would like to express my gratitude to my friends and the game Heart Stone, as they have brought immense joy and laughter to my daily life. I am thankful to Doctor Xiao, Doctor Yang, Doctor He, Doctor Wen, PhD Chen, PhD Wang, DCY,JYT,phD Wang and XY for their delightful presence and the wonderful moments we have shared together.

finally, I would like to convey my profound appreciation to my beloved family, including my parents and my younger sister. Their unconditional love and unwavering support have been my pillars of strength during challenging times. I feel immensely fortunate to be part of such a loving family, and I cherish the bond we share. My love for them is eternal, and I am forever grateful for their presence in my life.

TOHOKU UNIVERSITY

Abstract

Faculty of Agriculture

Graduate School of Agriculture

Doctor of Philosophy

Estimation of soil salinity and its effects on rice yield in Banphai, Northeast

Thailand

by YANG YI

Northeast Thailand is the majority rice cultivated area in Thailand, however its rice yield per hectare is lower than other rice cultivated regions. Soil salinity, derived from underground salt rock and accumulated by human activity, was considered the major rice yield limitation factor. This study focused on evaluating rice productivity related to salinity conditions and the application of UAV in Khon Kaen Province, Northeast Thailand. The field investigations were conducted from 2016 to 2019 in farmer fields in severe, moderate, and slight soil salinity classes determined by the Land Development Department of Thailand. The soil salinity on the basis of the electric conductivity of saturated soil extract (ECe) was not consistent with salinity soil classification by LDD, it seemed related with precipitation. Consequently, soil salinity affects on rice yield is not as serious as our initial imaginary. However, plenty of rainfall may have alleviated soil salinity and rice yield reduction in other years, causing differences in rice yield that were not significant among soil salinity classes. Using RGB images collected from UAV can efficiently estimate rice yield and rice growth, the medium of October around heading and flowering stage is the best stage to estimate rice yield by using RGB images-based vegetation index. Additional, using RGB images with machine learning method is also quite efficient to detect salinity conditions even in a very small farm.

Keywords: salinity, rice yield, soil moisture content, precipitation, UAV, RGB images, SVM, rice growth

Contents

| | |
|---|-------------|
| Abstract | iv |
| List of Figures | viii |
| List of Tables | xi |
| List of Abbreviations | xii |
| 1 General | 1 |
| 1.1 General introduction | 1 |
| 1.1.1 soil salinity | 1 |
| 1.1.2 Soil salinity impacts on rice | 3 |
| 1.1.3 Remote sensing in soil salinity mapping | 5 |
| 1.1.4 Climate change impacts on soil salinity in agricultural areas | 7 |
| 1.2 Purpose of study | 8 |
| 1.3 Organization of thesis | 8 |
| 2 Rice production in farmer fields in soil salinity classified areas in khon kaen, northeast Thailand. | 9 |
| 2.1 Introduction | 9 |
| 2.2 Materials and Methods | 10 |
| 2.2.1 Study area | 10 |
| 2.2.2 Field Investigations | 12 |
| 2.2.3 Weekly Measurement of Soil Salinity | 13 |
| 2.2.4 Rice Yield Measurement | 13 |

| | | |
|----------|--|-----------|
| 2.2.5 | Soil Measurement | 13 |
| 2.2.6 | Conversion of soil Solution EC and EC 1:5 to ECe | 14 |
| 2.3 | Results | 16 |
| 2.3.1 | Dynamics of Soil ECe and SMC among Classes from 2017 to 2019 | 16 |
| 2.3.2 | Effect of soil ECe and Moisture on Rice Yield | 18 |
| 2.3.3 | Rice Yield Based on Salinity Level at Harvest | 18 |
| 2.4 | Discussion | 21 |
| 2.5 | Conclusions | 22 |
| 3 | Evaluate rice growth and production in farmer fields under salinity stress by Unmanned Aerial Vehicle (UAV) RGB images in Khon, Kaen, Northeast Thailand. | 23 |
| 3.1 | Introduction | 23 |
| 3.2 | Materials and Methods | 25 |
| 3.2.1 | Study area | 25 |
| 3.2.2 | RGB images collection and Mosaic | 25 |
| 3.2.3 | Calculation of VIs | 27 |
| 3.2.4 | Algorithm of K-means cluster | 27 |
| 3.2.5 | Analysis of rice yield | 28 |
| 3.3 | Results | 28 |
| 3.3.1 | Estimating rice growth based on vegetation index by using UAV RGB images. | 28 |
| 3.3.2 | The relationship between rice yield and ExG on different rice growth stage. | 35 |
| 3.3.3 | Rice yield map based on RGB images. | 38 |
| 3.4 | Discussions | 39 |
| 3.4.1 | Conclusion | 42 |
| 4 | Yearly change in severely damaged areas in paddy fields in khon kaen,northeast Thailand. | 43 |

| | | |
|----------|----------------------------------|-----------|
| 4.1 | Introduction | 43 |
| 4.2 | Materials and methods | 44 |
| 4.2.1 | Study area | 44 |
| 4.2.2 | Measurement | 45 |
| 4.2.3 | Analysis | 46 |
| 4.2.4 | algorithm of SVM | 46 |
| 4.3 | Results and discussion | 47 |
| 4.4 | Conclusion | 53 |
| 5 | General | 54 |
| 5.1 | General discussion | 54 |
| 5.2 | General conclusion | 56 |
| | References | 57 |

List of Figures

| | | |
|-----|--|----|
| 1.1 | Soil salinity mechanisms | 2 |
| 1.2 | Plant respond under salinity stress | 4 |
| 2.1 | The investigated fields and locations on Google Maps. (a) Class 2. (b) Class 3. (c) Class 4. (d) Locations of study areas in Khon Kaen. Lines are the boundaries of the districts. | 11 |
| 2.2 | Rainfall during the investigated period from 2017 to 2019. The data were obtained from the meteorological station in Banphai. | 12 |
| 2.3 | Comparison between EC _e , EC 1:5, and ECs. (a) The relationship between soil EC _e and EC 1:5. (b) The relationship between soil EC _e and ECs. | 15 |
| 2.4 | Dynamics of soil EC _e in 2017 (a), 2018 (b), 2019 (c), and dynamics of soil moisture content (SMC) in 2018 (d). | 16 |
| 2.5 | Box plot of average EC _e of soil samples in the investigated period from 2017 to 2019. Diamond-shaped markers are outliers. The number of samples was 14 and 16 in class 2, class 3 in 2017; 10 and 10 in class 2, class 3 in 2018; 5 and 5 in class 2, class 4 in 2019, respectively. * significant at a probability level of 0.05 by the Mann–Whitney U test. | 17 |
| 2.6 | The relationship between average EC _e of soil samples during the investigated period and EC _e at harvest from 2017 to 2019. | 17 |
| 2.7 | The relationship between rice yield and EC _e at harvest from 2017 to 2019. | 18 |
| 2.8 | Box plot of rice yield among classes from 2017 to 2019. Diamond-shaped markers are outliers. ** significant at a probability level of 0.01 by the Mann–Whitney U test. | 19 |

| | | |
|------|---|----|
| 2.9 | Box plots of rice yield based on salinity level among classes in 2017(a); 2018 (b); 2019 (c). Diamond-shaped markers are outliers. NS (no saline): 0–2 dS m ⁻¹ ; LS (low salinity): 2–4 dS m ⁻¹ ; MS (mild salinity): 4–8 dS m ⁻¹ ; HS (high salinity): 8–16 dS m ⁻¹ ; SS (severe salinity): >16 dS m ⁻¹ . | 20 |
| 3.1 | The UAV:(a) DJI Phantom3 advanced;(b) DJI Mavic pro. | 26 |
| 3.2 | Experiment methodology and procedure of statistical analysis in this study | 28 |
| 3.3 | ExG of sampling points based on characteristic of k-means cluster in class 2 in 2018. | 29 |
| 3.4 | Boxplot of ECE (a) and yield (b) among clusters in class 2 in 2018. . . . | 30 |
| 3.5 | ExG of sampling points based on characteristic of k-means cluster in class 3 in 2018. | 31 |
| 3.6 | Boxplot of ECE (a) and yield (b) among clusters in class 3 in 2018. . . . | 32 |
| 3.7 | ExG of sampling points based on characteristic of k-means cluster in class 2 in 2019. | 33 |
| 3.8 | Boxplot of ECE (a) and yield (b) among clusters in class 2 in 2019. . . . | 34 |
| 3.9 | The R ² of the relationship between yield and ExG on different rice growth stage in 2018 (a) and 2019 (b). | 36 |
| 3.10 | The relationship between rice yield and ExG on the best R ² date in 2018 (a) and 2019 (b). | 37 |
| 3.11 | Rice yield map based on RGB images in class 2 in 2018 (a),in class 3 in 2018 (b),in class 2 in 2019 (c) and class 4 in 2019 (d). | 39 |
| 4.1 | The investigated fields on Google Maps. Circles show the investigated points for soil EC and rice yield in Figure 3 and 4, respectively. Rhombuses show the soil sampled points to support non-vegetated/vegetated analysis in Figure 5 and 6. EC and depth of ground water were measured with the field router. | 45 |
| 4.2 | Precipitation from 2016 to 2019 in Banphai. The numbers on the bars indicate precipitation amount between August and October. | 48 |

| | | |
|-----|--|----|
| 4.3 | Box plot of soil EC (1:5,soil:water) of investigated paddy fields from 2017 to 2019. The number of samples was 34,19 and 30 in 2017 ,2018 and 2019,respectively. The number to right of each symbols the EC,which exceeded 2.0 dS m^{-1} . Red symbols indicate the EC where the rice yield was 0 g m^{-2} | 49 |
| 4.4 | Box plot of rice yield of investigated paddy fields from 2016 to 2019. The number of samples was 29,34,19 and 30 in 2016,2017,2018 and 2019,respectively. | 50 |
| 4.5 | RGB images for the investigated areas at rice harvest in 2016,2018 and 2019. | 51 |
| 4.6 | Non-vegetated/vegetated classification for the investigated areas at rice harvest in 2016, 2018 and 2019. Red areas are classified as non-vegetated areas. Yellow and light blue rectangles are areas shown in Figure 7. | 51 |
| 4.7 | Changes in vegetation in RGB images in 2016,2018 and 2019 representative areas indicated in Figure 6 (above:yellow rectangle;below:light blue rectangle). | 52 |

List of Tables

| | | |
|-----|---|----|
| 1.1 | Criteria for classifying salinity of soils and crops growth based on FAO | 4 |
| 2.1 | ANCOVA result for rice yield by year, salinity, and class. | 20 |
| 3.1 | Characteristics and configuration of UAV utilization for data collection. | 26 |

List of Abbreviations

| | |
|---------------|---|
| LDD | Land Development Departure |
| ECs | Electricity Conductivity of soil Solution |
| EC | Electricity Conductivity |
| ECe | Electricity Conductivity of extract saturate paste |
| RS | Remote Sensing |
| SI | Salinity Index |
| NDSI | Normolized Difference Salinity Index |
| PLSR | Partial Least Squares Regression |
| SVM | Support Vector Machine |
| RF | Random Forest |
| CNN | Convolution Neural Network |
| ET | Evaporation Transportation |
| SMC | Soil Moisture Content |
| ANCOVA | ANalysis of COVAriance |
| UAV | Unmaned Aerial Vehicles |
| VI | Vegetation Index |
| NDVI | Normalized Difference Vegetation Index |
| ExG | Excess Greenness Index |
| ExG | Excess Greenness Index |
| TP | True Possitive |
| FP | False Possitive |
| TN | True Negetive |
| FN | False Negetive |

Chapter 1

General

1.1 General introduction

1.1.1 soil salinity

Soil salinity was defined as a high concentration of soluble salt in soil. It was the biggest agriculture problem associated with reducing crop productivity, corresponding a large economic lost with an annual global income loss of US\$27.3 billion [1]. 935 million ha area is affected by salt in the world [2]. Especially in arid and semi-arid region with more than 70% of this total salt-affected area, such as northeastern Asia, middle-East countries [3]. Moreover, it is expanding at the rate of 1-2 million ha per year [4] and the expanding speed tend to increase because of climate change [5]. The causes of soil salinity are general classified into primary and secondary salinity (fig1.1) [6]. The majority of salt-affected soils develop through primary salinity, which is a natural process occurring over an extended period of time due to the presence of saline rock materials or sediment [7]. Initially, chemical weathering processes release soluble salts from these parent materials [8]. These salts are then transported by water (surface streams or groundwater) and strong winds to arid and semi-arid regions, where low rainfall, high evaporation, and poor natural percolation cause the concentration of soluble salts to increase gradually, resulting in their deposition as secondary minerals in the soil [9]. On the other hand, secondary salinity is

attributed to human activities, particularly unsuitable irrigation, fertilization practices, and certain salt production industries. Poor water quality and inefficient agricultural management have led to saline damage in about 25% of the world's irrigated areas [10]. In regions like North Africa, Australia, and the Middle East, the extent of salt-damaged irrigation areas exceeds 50% [1]. In some water-scarce regions, farmers resort to using poor-quality water, including saline water, to meet crop water requirements, leading to approximately 18 million hectares of land being irrigated with strongly saline water worldwide [11], exacerbating soil salinity. Excessive irrigation with saline water, especially in areas with restricted soil drainage, raises the water table and causes subsequent evaporation of soil water, resulting in elevated soil salinity levels [12]. Additionally, the misuse and overuse of inorganic fertilizers contribute significantly to soil salinity buildup [13] [14]. These chemical fertilizers can alter soil pH, affect the availability of certain ions, and ultimately increase soil salinity [15]. Proper management and understanding of the causes of soil salinity are essential for sustainable agricultural practices and to mitigate the negative impacts on crop productivity and soil health.

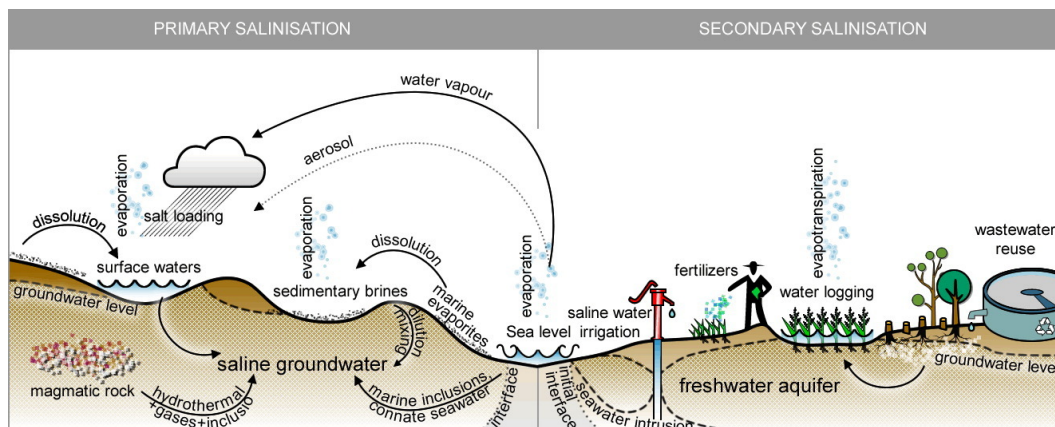


FIGURE 1.1: Soil salinity mechanisms

Soil salinity is typically assessed by measuring the electrical conductivity (EC) of soluble salt concentrations in the soil water. The primary soluble mineral salts include cations such as sodium (Na^+), calcium (Ca^{2+}), magnesium (Mg^{2+}), potassium (K^+), and anions like chloride (Cl^-), sulfate (SO_4^{2-}), bicarbonate (HCO_3^-), carbonate (CO_3^{2-}), and nitrate (NO_3^-). The widely accepted standard for defining saline

soil is based on the electrical conductivity of the soil extract obtained from a saturated paste (EC_e) at 25 degrees Celsius, which should be equal to or exceed 4 deci Siemens per meter (dS m⁻¹) [16]. However, obtaining the soil saturation extract from soil paste can be challenging and often relies on the experience of the personnel conducting the measurement. To address this, field investigations commonly measure the EC of extracts using different soil-to-water ratios (1:5, 1:2.5, 1:1) as alternative approaches to assess soil salinity.

1.1.2 Soil salinity impacts on rice

The impact of salinity on plants can be broadly categorized into two types of stress: osmotic stress and ionic stress (figure 1.2). In the early stages of exposure to high salinity, the concentration of salt outside the root inhibits water uptake, cell expansion, and lateral bud development [17]. As salinity persists, the accumulation of ions exceeds the plant's tolerance threshold, leading to wilting and death of leaves and a subsequent decrease in the activity of essential cellular processes, including photosynthesis [18]. The response of crops to salinity varies depending on the species. Generally recognized soil salinity and its effects on crop plants are given in (table 1.1)

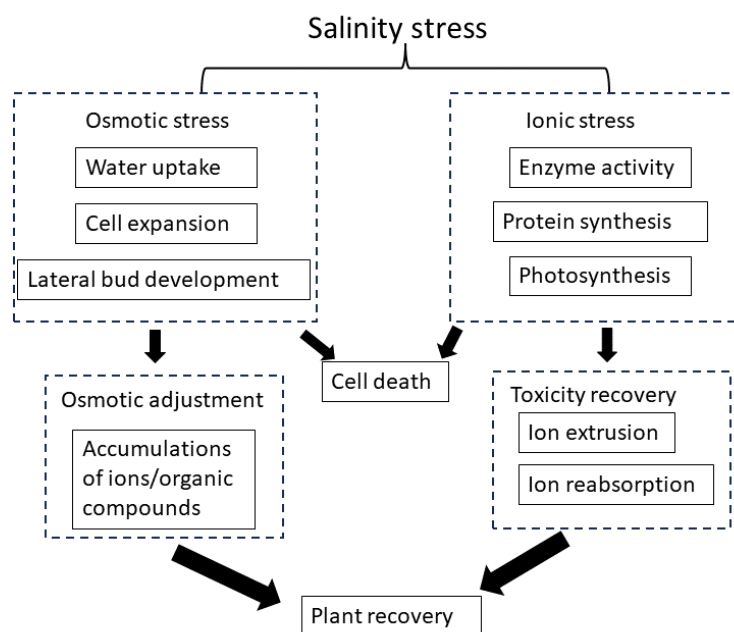


FIGURE 1.2: Plant respond under salinity stress

TABLE 1.1: Criteria for classifying salinity of soils and crops growth based on FAO

| Saline soil levels | ECe (dS m ⁻¹) | Effect on crops |
|--------------------|---------------------------|---|
| None saline | 0-2 | Salinity effects negligible |
| Slightly saline | 2-4 | Yield of sensitive crops may be restricted |
| Moderately saline | 4-8 | Yield of many crops are restricted |
| High saline | 8-16 | Only tolerant crops satisfactorily |
| Very highly saline | >16 | Only a few very tolerant crops yield satisfactorily |

Rice is the most sensitive salinity response cereal [17], specifically, at the early vegetative and later reproductive stages [19]. Rice salinity tolerance varied with

genotypes because of additive gene effects [20]. A previous research revealed that rice is more resistant at reproductive and grain filling stage than germination and vegetative stages [21]. However, some research also reported that low salinity level can increase the resistant of rice to higher and lethal salinity levels [22]. According to previous researches, salinity is the second type of stress and is the most predominant hindrance to rice production after drought [23]. Previous studies indicated that the negative affection of soil salinity to rice can be described through the piecewise linear salt tolerance equation [24].

$$Y_r = 100 - b * (EC_e - a)$$

where Y_r represents the relative rice yield, EC_e is electrical conductivity of the saturation extract ($dS\ m^{-1}$), a is the salinity threshold ($dS\ m^{-1}$) and b is the slope expressed as % per $dS\ m^{-1}$.

Besides, previous studies showed that most rice were cultivated under the moderate saline (EC_e 4-8 $dS\ m^{-1}$) and highly saline (8-16 $dS\ m^{-1}$) soils [25]. Under this saline condition, rice production was reduced significantly with an almost 50% reduction [26][27]. Considering rice's vulnerability to salinity stress, it becomes crucial to explore and implement strategies that can enhance its tolerance and productivity under saline conditions. Efforts to develop salt-tolerant rice varieties through breeding and genetic research are vital for ensuring food security and sustaining rice production in regions affected by salinity. Additionally, adopting proper agricultural practices and management techniques tailored to salinity-prone areas can further mitigate the negative impact of salinity on rice cultivation.

1.1.3 Remote sensing in soil salinity mapping

Regular and accurate monitoring of soil salinity is essential to mitigate its adverse effects on agriculture and the environment. However, traditional monitoring techniques are time-consuming, labor-intensive, and limited to specific locations for relatively short durations. To overcome these limitations and make informed decisions,

the adoption of advanced procedures and techniques for soil salinity monitoring becomes crucial [28]. Remote sensing (RS) technology has proven to be effective for salinity mapping, as demonstrated in numerous previous studies [29][30]. RS imagery is particularly well-suited for mapping the surface expression of salinity [31]. Often, a sparse cover of vegetation can serve as an indicator of salinity in many cases. The global aim of such endeavors is to assess and map soil salinity, leading to a better understanding of the problem. This, in turn, allows for the timely and reliable provision of information, enabling the implementation of necessary solutions to prevent an increase in salinization in new areas or to reduce salinization in existing areas. By leveraging remote sensing techniques, it becomes feasible to address soil salinity challenges more efficiently and make informed decisions to safeguard agricultural productivity and the environment.

Normally, remote sensing technology can be divided into two types based on the platform: the one is satellite-based remote sensing and the other one is UAV-based technology. Satellite-based technology has provided cost-effective, fast, quantitative information on saline soil in a relative large scale, such as in county, district and city [32][33]. The most commonly used multispectral satellite remote sensing data source for soil salinity estimation was Landsat with 16-day revisit period due to free accessory and the relative higher resolution of 30m [34][35]. While, sentinel-2 has a higher resolution of 10-20 m and a shorter revisit period with 5 days [36]. Compared with sentinel-2 and Landsat, MODIS data is also commonly used due to its own advantages of smaller time granularity to capture salinity dynamics [37]. The NIR and SWIR of these data source are considered effective to distinguish the spectrum of saline soil [38] [39]. The limitations of these satellite remote sensing methods can be attributed but not limited to the relatively low resolution. Some hyperspectral and resolution satellite-based data resource can solve these disadvantages, but it may limit their large scale applications due its high cost. Besides, radar microwave satellite-based imagery, such as sentinel-1 backscatter data, is also effective to estimate soil salinity [40] [41], which currently has showed its advantages in soil moisture retrieval [42]. UAV-based remote sensing technology integrate the power of GPS position, telemetry, remote control, and advanced remote sensing techniques

to achieve the intelligent and swift acquisition, processing, and analysis of the high-resolution imagery data. According on the spectral characteristics of soil salinity. A lot of salinity indices such as Salinity Index 1-Salinity Index 6 (SI1-SI6) and the normalized difference salinity index (NDSI) have been established [43] [44]. The research concluded that the recognition effect of the integrated band (covering the visible-near-infrared band and the combined band in the infrared spectral range) is superior to that of the independent band, and most of the vegetation index can be used as an estimation index of soil salinity content to reflect soil salinity indirectly [45] [46]. Additional, a lot of algorithm such as multilinear regression method, partial least squares regression (PLSR), support vector machine (SVM), Random forest (RF) and convolutional neural network (CNN) were used to quantitative estimation soil salinity. However, the soil salinity sensitive of different indices has strong regionality [47] [48].

1.1.4 Climate change impacts on soil salinity in agricultural areas

In the past several hundred years, climate change has been noticed in a lot fields, especially in agriculture because it is significant impact soil properties, surface waters and stream waters which is important for agriculture [49] [50]. It was defined by increasing atmospheric CO₂; increasing air temperature; abrupt and large varied in daily, seasonal and annual temperature; intensive rainfall events; changes in wet and dry cycles and so on. previous study indicated that the climate change can affect primarily rainfall, potential evapotranspiration and temperature [51]. In addition, increased global temperature can also raise ocean levels and will bring more extremely weather conditions. Droughts and flooding are expected to increase in frequency and intensity. Hot dry areas are expected to become hotter and drier, some wet areas wetter, cold areas will be colder. Changes in the frequency and intensity of rainfall, temperature and other extreme weather events will impact agricultural productivity, with the negative affection [52].

Climate change patterns influence the salinization process. Abundant or limited rainfall can be significant impacts on soil salinity in the root zone [53] [54]. Abundant rainfall raises the water table, this results in the accumulation of salinity at or

near the soil surface during the dry portion of the year when insufficient rainfall is available to leach the salts from the root zone. On the contrary, during the rare rainfall year, water moves upward from the shallow water table due to ET. As a consequence of changes in climate patterns, salt accumulation is most likely to happen in irrigated agricultural areas around the world subjected to extended drought conditions where shallow water tables and fine textured soil exist and in areas subjected to extensive rainfall where salinity accumulates due to upslope recharge and downslope discharge or where shallow water tables and fine-textured soils exist.

1.2 Purpose of study

To evaluate soil salinity impacts on rice growth and productivity using UAV RGB images. There are three purposes in this study: (1) Investigate salinity condition and yearly change of severe salinity condition in rainy season in study area; (2) Assess the impact of salinity on rice productivity; (3) Assess the application of UAV technology in detecting salinity conditions and yield estimation.

1.3 Organization of thesis

In chapter 2, the field investigations for rice yield and soil salinity conditions in rainy season over three years was demonstrated. To evaluate soil salinity, E_{Ce} of soils were measured. And the relationship between rice yield and E_{Ce} was also examined. In chapter 3, to assess rice growth and yield using UAV, VIs were calculated from RGB images, k-means clustering method was employed to group rice growth, and the relationship between VIs and rice yield at different rice growth stage was also verified. Chapter 4 demonstrated the very severe salt-damaged area change with years over 4 years, non-vegetated areas were assumed to be the severe salt-damaged areas, machine learning method (SVM) method was used to detect the non-vegetated areas on RGB images. Finally, Chapter 5 summarizes all analysis results and discusses the effects of salinity on rice growth and productivity.

Chapter 2

Rice production in farmer fields in soil salinity classified areas in khon kaen, northeast Thailand.

2.1 Introduction

Soil salinity is a major agricultural problem in global crop production [55], and it has accounted for approximately 20% of the world's cultivated area [56]. Furthermore, soil salinity is expected to increase because of climate change in the future, and some researchers have reported that serious salinization may increase up to 50% of all arable land by 2050 [57]. Most salinity-affected soil areas are located in Africa and Asia, especially in southeastern Asia [58]. For example, in Northeast Thailand, approximately 17% of the land is affected by salt [59]. The resource of salinity is an underground salt rock in Northeastern Thailand [60]. Moreover, soil salinity has accumulated from human activities, such as irrigation, deforestation, and salt manufacture [61]. To evaluate the soil salinity situation in Northeast Thailand, the Land Development Department (LDD) classified soil salinity into four classes according to the salty crust in the dry season: class 1 "very severely" (salt crust > 50%), class 2 "severely" (salt crust 10–50%), class 3 "moderately" (salt crust 1–10%), and class 4 "slightly" (salt crust < 1%).

Rice is the most important crop in Northeast Thailand [62]. The cultivated area

occupies more than 50% of the total rice cultivated area in Thailand, but the yield per hectare is the lowest among regions [63]. Although poor soil fertility and low water availability are the major constraints of production with extensive management [64], soil salinity has caused serious problems in some areas [65].

Rice is highly sensitive to salinity compared with other crops [66]. The responses to salinity are often represented by indicators such as NaCl concentration and electric conductivity (EC) [67][68]. The electric conductivity of saturated soil extract (ECe) is one of the representative indicators and is used to describe salinity levels by the USDA [69]. Maas and Grattan [70] pointed out that rice yield is significantly reduced by soil salinity over 3 dS m^{-1} ECe. However, the above-mentioned soil salinity classes classified by LDD do not correspond to ECe and rice productivity. The soil salinity conditions in relation to rice production have also been insufficiently reported [71]. Therefore, we conducted field investigations to evaluate salinity conditions and rice production in salt-affected areas in Khon Kaen province, Northeast Thailand. We selected the study area based on the soil salinity classification by LDD. The salinity condition was evaluated on the basis of ECe. Based on the analysis of the relationship between salinity condition and rice production, we discussed the classification method of salinity level and further strategies to alleviate salinity damage.

2.2 Materials and Methods

2.2.1 Study area

The study area (Figure 2.1), located in Khon Kaen, Northeast Thailand, is characterized as having a tropical savanna climate with two seasons (rainy and dry seasons) with an average annual precipitation of approximately 1100 mm. In this area, jasmine rice (KDML 105), is widely cultivated. Farmers plant rice once a year in the rainy season, sow rice in June or July, and harvest in early or mid-November. We conducted field investigations from August to November every year from 2017 to 2019.

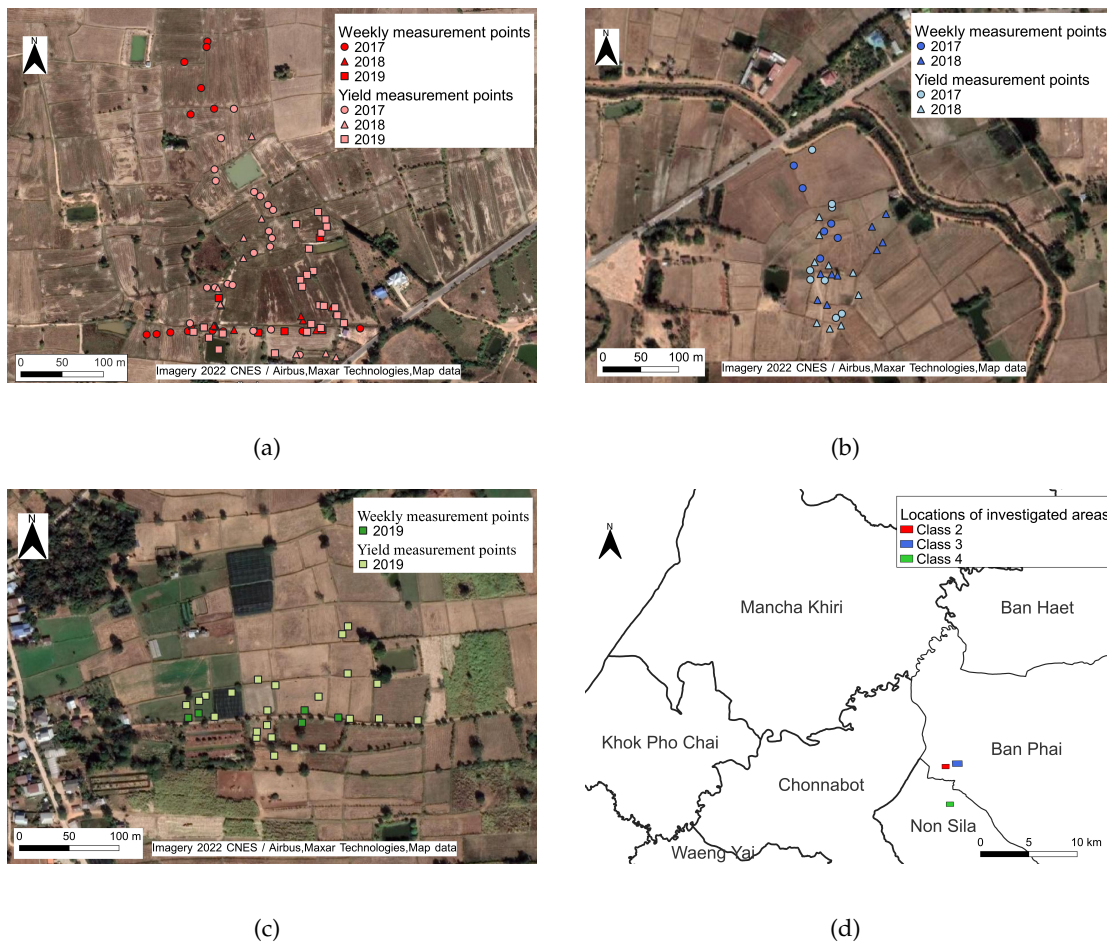


FIGURE 2.1: The investigated fields and locations on Google Maps. (a) Class 2. (b) Class 3. (c) Class 4. (d) Locations of study areas in Khon Kaen. Lines are the boundaries of the districts.

Precipitation data were obtained from the meteorological station in the Banphai, Meteorological Department, which is the nearest meteorological station to the study area. Precipitation in the investigated period varied from year to year (Figure 2.2). The amounts in 2018 and 2019 were less than half of that in 2017. The amounts were similar between 2018 and 2019, but the patterns were different: the rainfall level was high in June and July in 2018 but high in August and September in 2019.

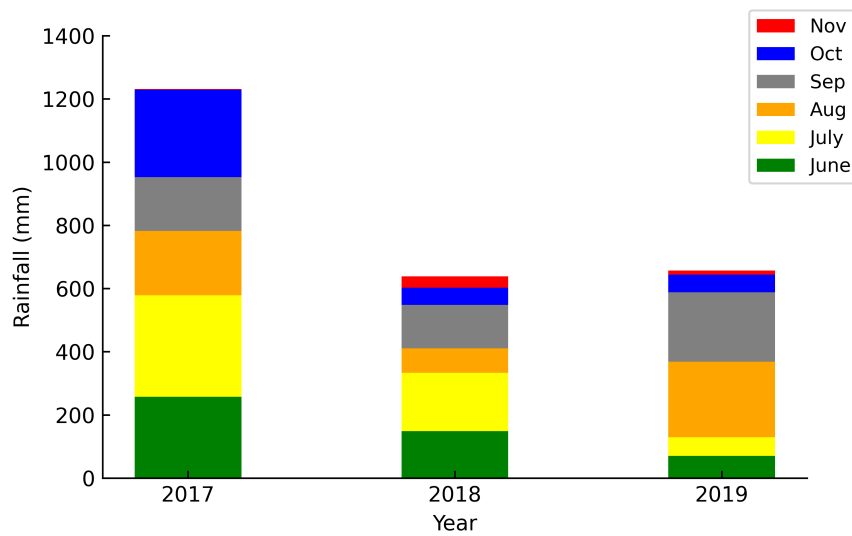


FIGURE 2.2: Rainfall during the investigated period from 2017 to 2019. The data were obtained from the meteorological station in Banphai.

2.2.2 Field Investigations

Field investigations were conducted in classes 2 and 3 in 2017 and 2018. The areas followed the classification of the LDD [72]. Since farmers in class 3 did not plant rice in 2019, due to the drought correct in June and July 2019 following crop failure in 2018, we conducted an investigation in class 4. The investigations were divided into 2 measurements: one was the weekly measurement of soil salinity, and the other was rice yield measurement. The weekly measurement of soil salinity was conducted at 14 and 6 points in 7 and 3 fields in class 2 and class 3 in 2017, 10 and 10 points in 5 and 5 fields in class 2 and class 3 in 2018, and 5 and 5 points in 5 and 5 fields in class 2 and class 4 in 2019, respectively (Figure 2.1). The points were selected to represent the classification area. We tried to investigate the same fields for 3 years but failed because some fields were not planted. The measurement was conducted from August 29 to November 5, from September 11 to November 6, and from October 8 to November 13 in 2017, 2018, and 2019, respectively. The rice yield measurement was conducted at 34 and 14 points in class 2 and class 3, 19 and 19 points in class 2 and class 3, and 30 and 26 points in class 2 and class 4, respectively, which included the points of the weekly measurement of soil salinity. The points were selected to

compensate for the weekly measurement points. The rice was harvested for measurement on November 5 in 2017, November 6 in 2018, November 8 in class 4, and November 13 in class 2 in 2019, respectively.

2.2.3 Weekly Measurement of Soil Salinity

A soil solution sampler (DIK-301B, Daiki Rika Kogyo Co., Ltd., Saitama, Japan) was installed at 10 cm depth at each weekly measurement point to collect soil solution. A total of 10 mL of soil solution was collected weekly for EC measurement (ECs). When the soil solution was not extracted due to drought, 450 g of soil sample was collected from the surface to 12 cm depth around the weekly measurement point (within a radius of 1 m). The soil was subjected to EC 1:5, E_{Ce}, and moisture content measurements.

2.2.4 Rice Yield Measurement

Rice plants were harvested in a circle with an area of 1 m² at each point. The yield was determined with rough grain calibrated with a moisture content of 14%. A total of 450g of soil sample was collected from surface to 12 cm depth and subjected to EC 1:5 and E_{Ce} measurements. Soil salinity level was classified by E_{Ce} based on US Salinity Laboratory Staff [69]: NS (none saline): 0–2 dS m⁻¹; LS (low salinity): 2–4 dS m⁻¹; MS (mild salinity): 4–8 dS m⁻¹; HS (high salinity): 8–16 dS m⁻¹; SS (severe salinity): >16 dS m⁻¹.

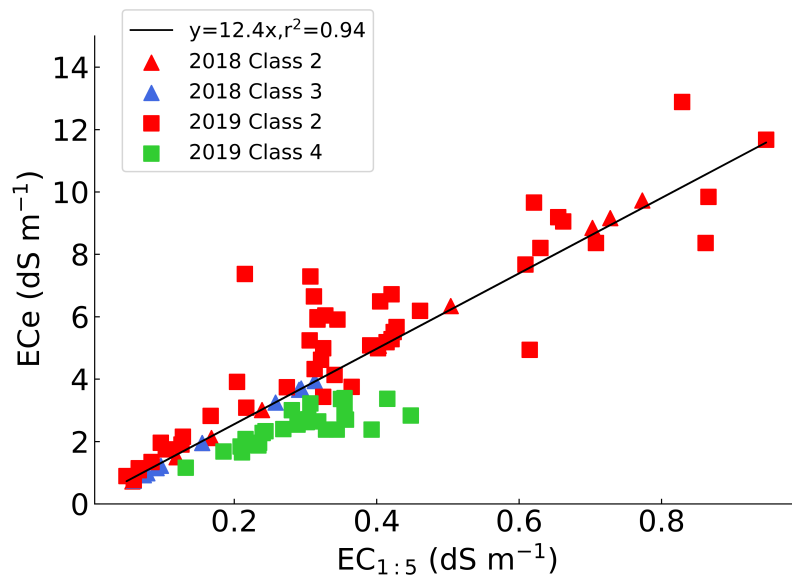
2.2.5 Soil Measurement

The moisture content of soil samples was determined by the ratio of the soil weight before drying and after drying. Air-dried soil samples were passed through a 2 mm sieve. EC of saturated paste (E_{Ce}) was determined using the methods outlined by the USDA [69]. The saturated paste was prepared by adding distilled water to 350 g soil samples and stirred until saturation. The saturated paste was left for 24 h for equilibration. The saturated paste extracts were obtained by using a Bucher Funner and applying suction. A 1:5 soil–water suspension was prepared to determine EC 1:5 by adding 50 g of distilled water to 10 g of air-dried soil. E_{Ce}, EC 1:5, and soil

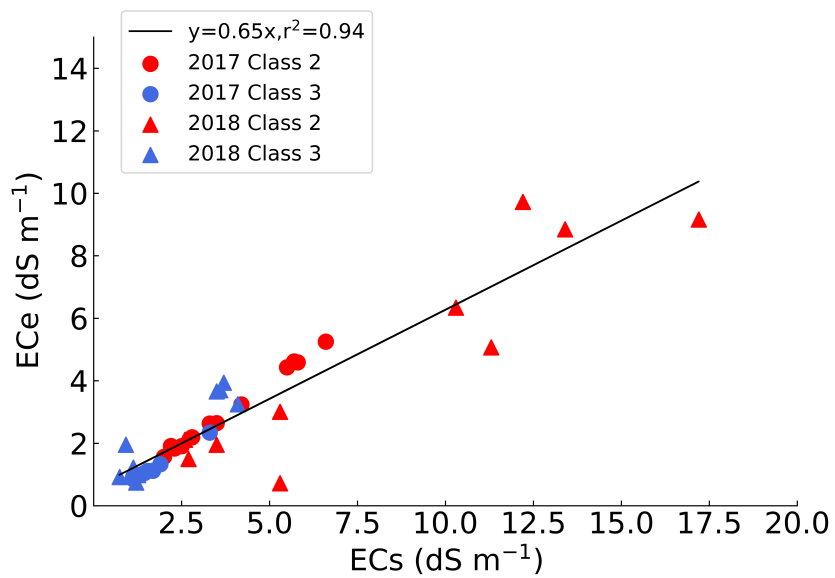
solution EC (ECs) were determined by an EC meter (FiveEasyTM Plus EC meter FEP30, Mettler Toledo, Greifensee, Switzerland).

2.2.6 Conversion of soil Solution EC and EC 1:5 to EC_e

EC_e had strong linear relationships with soil EC 1:5 and ECs (Figure 2.3). Although EC 1:5 in class 4 in 2019 had a lower EC_e, and the regression lines with 0 intercepts were applied to convert EC 1:5 and ECs to EC_e in this study.



(a)



(b)

FIGURE 2.3: Comparison between ECe, EC 1:5, and ECs. (a) The relationship between soil ECe and EC 1:5. (b) The relationship between soil ECe and ECs.

2.3 Results

2.3.1 Dynamics of Soil ECe and SMC among Classes from 2017 to 2019

The dynamics of soil ECe varied among years (Figure 2.4). A higher ECe was observed in the drought year 2018. ECe was rather stable in 2017 and 2019. The average ECe in class 2 was higher than that in class 3, but ECe in class 2 was not always higher than that in class 3 in some fields. Class 4 showed a relatively higher ECe than class 2, especially on 8 and 14 October 2019. Soil moisture content (SMC) was obviously lower in class 3 than in class 2 in 2018. An SMC decrease, which was unable to extract soil solution, rarely occurred in 2017 and 2019. Although the relationship was not clear, ECe tended to increase under low SMC after 10 October 2018.

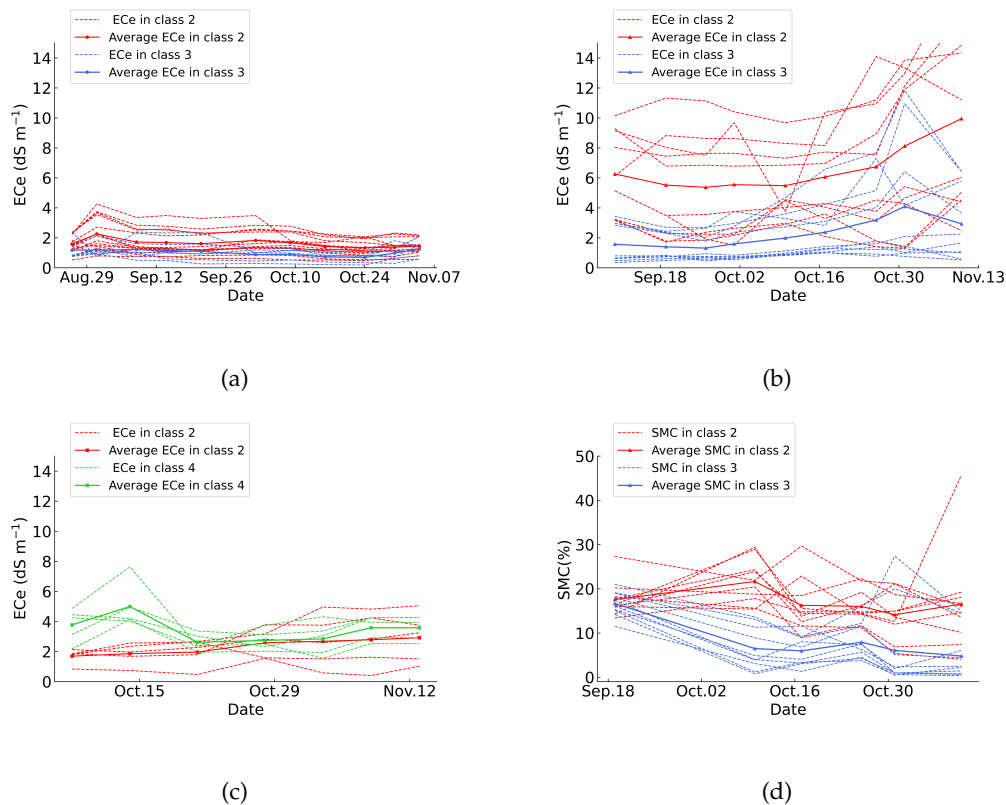


FIGURE 2.4: Dynamics of soil ECe in 2017 (a), 2018 (b), 2019 (c), and dynamics of soil moisture content (SMC) in 2018 (d).

The average ECe of the weekly measurement at each measurement point showed large variation only in 2018 (Figure 2.5). The ECe in class 2 was significantly higher than that in class 3 in 2018. However, a significant difference was not observed between class 2 and class 3 in 2017, or between class 2 and class 4 in 2019.

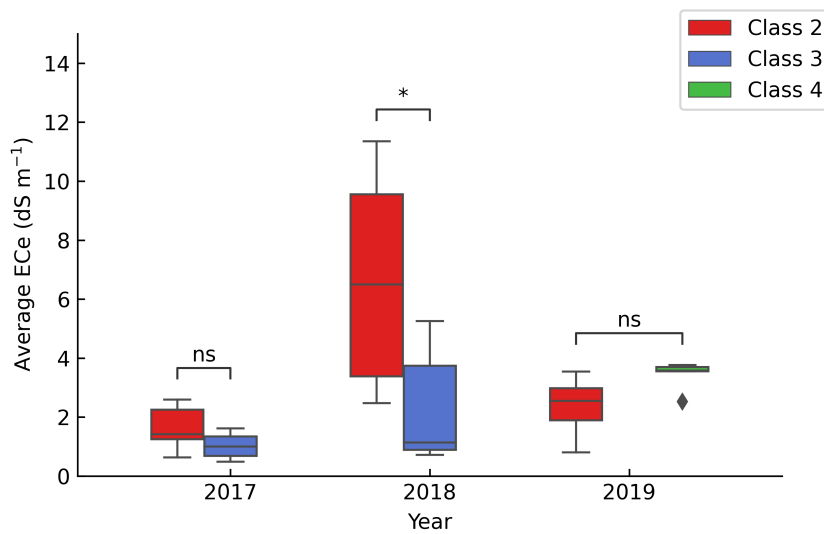


FIGURE 2.5: Box plot of average ECe of soil samples in the investigated period from 2017 to 2019. Diamond-shaped markers are outliers. The number of samples was 14 and 16 in class 2, class 3 in 2017; 10 and 10 in class 2, class 3 in 2018; 5 and 5 in class 2, class 4 in 2019, respectively. * significant at a probability level of 0.05 by the Mann-Whitney U test.

Soil ECe at harvest has a linear positive relationship with average ECe of weekly measurement (Figure 2.6). Accordingly, the soil ECe at harvest was used to classify the soil salinity level in the following analysis.

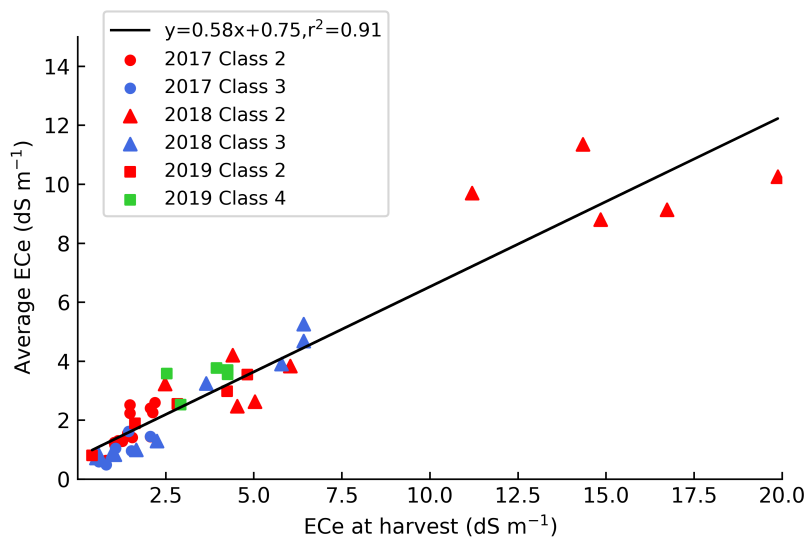


FIGURE 2.6: The relationship between average ECe of soil samples during the investigated period and ECe at harvest from 2017 to 2019.

2.3.2 Effect of soil ECe and Moisture on Rice Yield

Figure 2.7 shows the relationship between rice yield and ECe at harvest. An extremely low rice yield ($<100 \text{ g m}^{-2}$) was observed where ECe was higher than 10 dS m^{-1} in class 2 in 2018. The extremely low rice yield was also observed where ECe was lower than 6 dS m^{-1} in class 3 in 2018. The fields that showed low rice yield in class 3 in 2018 corresponded to those that had a low SMC (Figure 2.4). Except for the extremely low rice yield, rice yield varied among points and did not show any tendency against ECe.

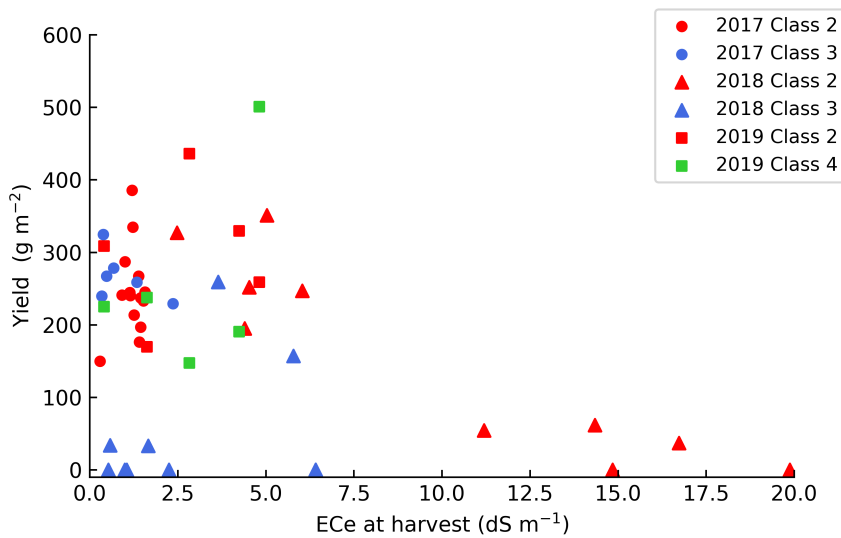


FIGURE 2.7: The relationship between rice yield and ECe at harvest from 2017 to 2019.

2.3.3 Rice Yield Based on Salinity Level at Harvest

The rice yield measurement showed that yield reduced only in class 3 in 2018, and was not significantly different between classes in 2017 and 2019 (Figure 2.8). The lower yield in class 3 in 2018 might have been caused by the low SMC (Figure 2.4). Rice yield varied in a large range even at the none saline and low soil salinity level (Figure 2.9). However, the median yield tended to decrease with increasing salinity levels. Analysis of covariance showed that the effects of salinity levels and year were significant but that of class was not significant (Table 2.1).

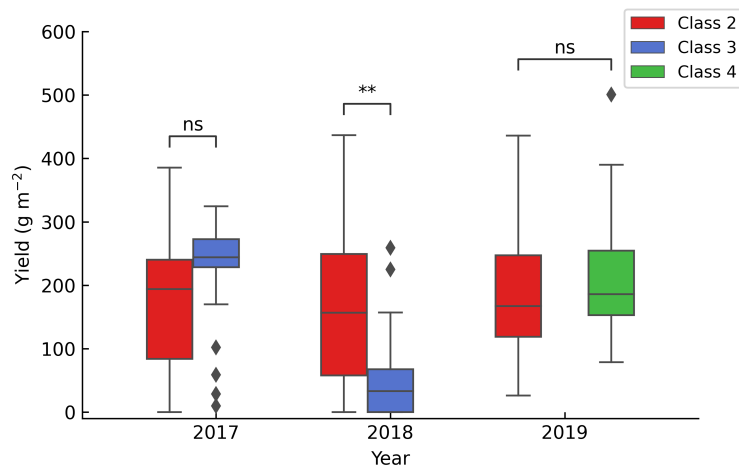


FIGURE 2.8: Box plot of rice yield among classes from 2017 to 2019. Diamond-shaped markers are outliers. ** significant at a probability level of 0.01 by the Mann–Whitney U test .

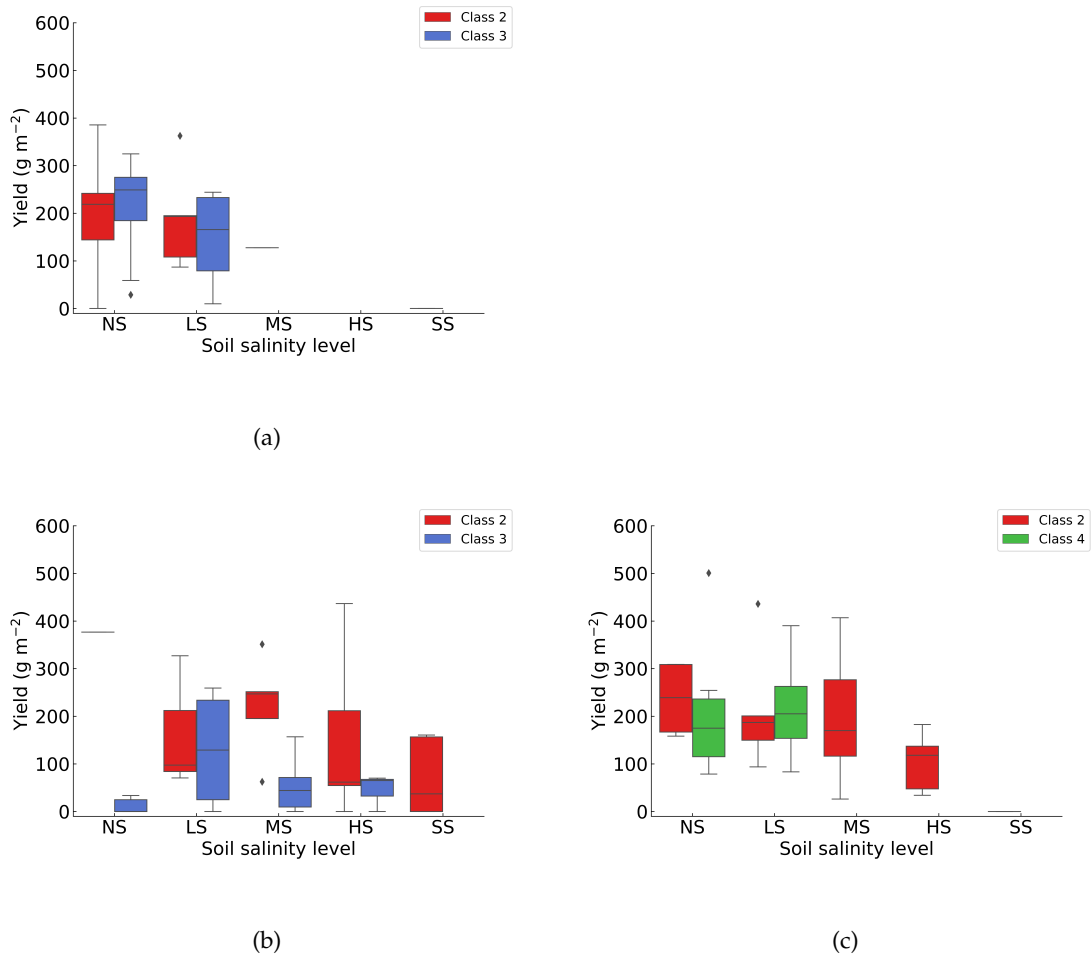


FIGURE 2.9: Box plots of rice yield based on salinity level among classes in 2017(a); 2018 (b); 2019 (c). Diamond-shaped markers are outliers. NS (no saline): 0–2 dS m⁻¹; LS (low salinity): 2–4 dS m⁻¹; MS (mild salinity): 4–8 dS m⁻¹; HS (high salinity): 8–16 dS m⁻¹; SS (severe salinity): >16 dS m⁻¹.

TABLE 2.1: ANCOVA result for rice yield by year, salinity, and class.

| Source | F Value | p Value |
|----------------|---------|----------|
| Year | 6.41 | 0.002 ** |
| Salinity level | 10.41 | 0.002** |
| Class | 1.74 | 0.189 |

** Significant at a probability level of 0.01.

2.4 Discussion

Soil salinity varied from year to year, which seemed to be associated with precipitation. The low precipitation in August and September of 2018 decreased SMC and increased E_{Ce}, which caused significant differences in E_{Ce} between classes 2 and 3. However, abundant rainfall alleviated E_{Ce}, which resulted in no significant difference among classes. The LDD defined classes based on salt crust in the dry season, but the results in this study suggest that another classification is required for rice production in the rainy season. Precipitation is generally more than potential evapotranspiration in the rainy season, but in 2018 it was less [73]. Including climate data is necessary for the classification. Yang et al. [74] reported that no vegetation areas due to severe salt damage were partly distributed in class 2. The detailed mapping of soil salinity is also required [75].

The soil salinity level based on soil E_{Ce} suggested that rice yield was damaged by soil salinity (Figure 2.9). E_{Ce} could be a candidate indicator of soil salinity mapping for rice production if the value was predictable in the rainy season. However, rice yield varied in a large range even at the same salinity level, obscuring the relation between rice yield and E_{Ce} (Figure 2.4). This fact, on the contrary, implies that farmer management could alleviate salinity damage. Farmers can obtain higher yields even at high and severe salinity levels. Since farmers partly applied irrigation water with a small water pump, effective irrigation may directly reduce the salinity level in addition to drought. Cost and water availability are the major limiting factors in the region [76][77]. Development of salinity level management with water-saving culture is recommended. The salinity level of irrigation water also needs to be checked [78]. Since the attainable rice yield of KDML 105 is 450 g m⁻² [79][80], the yield can be improved. Proper nutrient management may be necessary because low soil fertility due to light-textured soil is generally considered a yield constraint [81]. The authors also observed severe lodging in some locations due to excess stem growth. Control of rice growth is also recommended. Homma et al. [64] suggested that optimization of fertilizer application produces higher productivity by reducing fertilizer at the earlier planted field and increasing fertilizer at the later planted field. Nutrient management based on leaf color may be effective [82].

Although the expansion of severely salt-damaged areas was not observed [74], increases in soil E_c are predicted in the study area in the future [73]. Higher potential evaporation under global warming conditions may produce more severe salinity conditions [83, 84]. Several attempts were tested to alleviate soil salinity [85, 86]. Since deforestation is one of the major causes that enhances the salinity problem in the region, ecological management is also considered for the countermeasures [87, 88]. One of the major countermeasures is reducing the groundwater level in the dry season by tree planting. The lower groundwater level is expected to prevent salinity movement from the deep soil layer to the surface. However, a strategy has not been developed to reach a solution. Under this situation, the spatial and temporal evaluation of salinity conditions is primarily recommended. The evaluation may provide a local solution to continue rice production in the salinity classified area.

2.5 Conclusions

This study conducted field investigations to evaluate rice production in relation to salinity conditions, where the LDD classified soil salinity. Soil salinity in terms of E_c was affected by the precipitation amount and was not always consistent with the classes by LDD. The salinity level based on E_c was a more suitable indicator to evaluate the salinity damage of rice. These results suggest that the spatial and temporal evaluation of salinity conditions based on E_c is required for rice production. Large yield variation even at high and severe salinity levels suggests that rice yield can be improved by farmer management. Since deterioration of salinity conditions is anticipated under future climate change, further investigation is recommended to alleviate salinity damage for rice production.

Chapter 3

Evaluate rice growth and production in farmer fields under salinity stress by Unmanned Aerial Vehicle (UAV) RGB images in Khon, Kaen, Northeast Thailand.

3.1 Introduction

Improve crop production, satisfied the increasing demand for agricultural products with expansion of world population, is one of the greatest challenges of 21st century [89]. Rice, a staple food for more than 3 billion people, is an import crop for global food security [90]. Timely and accurate rice estimation are vital for precision management, policy and marketing decisions [91]. A traditional way of collect rice yield data involved labor-intensive and time-consuming field surveys and destructive sampling at various scales, which often resulted in significant uncertainties [92]. Alternatively, certain rice yield estimation models have been developed to provide accurate estimates while saving time [93]. However, model needs to calibrated with

a lot parameters, such as soil property, phenological period, fertilizer application and so on [94].

With development of technology, remote sensing has been become possible to predict rice yield, and satellite-based remote sensing has achieved a high level of prediction accuracy [95] [96]. however, the low resolution, high cost, and easy effected by weather condition during the rice growth period of satellite-based remote sensing limit data acquirement [97]. Moreover, many previous studies reported that satellite-based remote sensing can only provide a high accuracy of rice yield prediction at a large scale such as country, province or county [98] [99], but they are not possible to describe the detailed yield variation at a relatively small scale especially the average rice farm size is relatively smaller in northeast Thailand than other countries [100]. The recent increase in availability of unmanned aerial vehicles (UAV) are potential to increase temporal image data acquisition with high spatial resolution. The vegetation index (VIs) calculated from UAV-based images have proven to be well-established method for rice prediction. [101] used the VIs calculated from UAV-based RGB images to assess wheat yield from the heading stage to the mature stage. However, most researchers were focus on employ multispectral or hyperspectral UAV platform to rapidly estimate crop yield [102]. The previous paper reported that normalized difference vegetation index (NDVI) is highly related with the grain yield in wheat at the filling stage [103] [104]. The combination of Vis, calculated from RGB and multispectral images, were also utilized to assess yield in barley at the booting stage [105]. These mentioned studies proved that use of appropriate VIs can predict yields compared to traditional methods more efficiently.

Since using of multispectral and hyperspectral images are difficult to apply in the real farm cultivation due to the high cost and difficult utilizations. RGB images has advantages in budget with the acceptable accuracy. The objectives of this study including :1) estimate rice growth by using VIs from RGB images in salinity conditions; 2) estimate the relationship between rice productivity and VIs at different rice growth stage; 3) make spatial rice yield distribution map on basis of RGB images.

3.2 Materials and Methods

3.2.1 Study area

The study area and sampling points are the same with chapter 1 (2.1) in class 2, class 3 in 2018, class 2 and class 4 in 2019, respectively.

3.2.2 RGB images collection and Mosaic

The collection of RGB image data using UAVs was conducted on various dates, including September 10th, 19th, and 26th, October 3rd, 10th, 17th, 26th, and 31st in 2018 for class 2 and class 3. Additionally, data collection took place on October 8th, 14th, and 21st, November 8th in 2019 for class 2 and class 4. The data collection spanned from the heading stage to the harvesting stage. The heading stage is a crucial growth phase in rice production as it signifies the transition from vegetative to reproductive growth and is highly sensitive to temperature [106]. Details about the characteristics and configurations of the aerial data acquisition by UAV can be found in Table (3.1). The RGB images were captured using UAVs (3.1), namely "DJI Phantom3 advanced " and "DJI Mavic Pro," equipped with RGB cameras in the respective years of 2018 and 2019. To mitigate the impact of time of day and solar elevation angle on passive reflectance sensor measurements [107], the RGB image data collection using UAV was conducted around noon, between 11:00 am and 1:00 pm, on cloud-free and sunny days. The UAV flew at an altitude of 50 meters above ground level, ensuring an 85% forward and side overlap rate. The image processing software 'Pix4D mapper' (Pix4D, Lausanne, Switzerland) was employed to generate mosaic images from the RGB data. The mosaic images were used to do georeference based on google map. Initially, the RGB bands were converted into normalized forms using the following Equation:

$$R = r / (r + g + b)$$

$$G = g / (r + g + b)$$

$$B = b / (r + g + b)$$

where r, g, b are the original RGB digital values. Then, the original values are converted into values that range from 0 to 1, so that the normalized values can better represent the quantitative analyses in remote sensing domains.



(a)



(b)

FIGURE 3.1: The UAV:(a) DJI Phantom3 advanced;(b) DJI Mavic pro.

TABLE 3.1: Characteristics and configuration of UAV utilization for data collection.

| Source | 2018 | 2019 |
|-----------------|-------------------------|--------------------|
| Flight time | 11:00 am 13:00 pm | 11:00 am 13:00 pm |
| Flight date | 10,19,26 Sep,3,10,17,26 | 08,14,21 Oct,8 Nov |
| Flight altitude | 50 m | 50 m |
| overlap rate | 85% | 85% |

3.2.3 Calculation of VIs

Based on previous researches [108] [91], numerous vegetation indices (VIs) have been proposed to effectively correlate with rice yield and growth. In this study, we selected the Excess Greenness Index (ExG) as the VI of interest, which is calculated based on the red (R), green (G), and blue (B) bands of the spectral data. ExG is widely utilized in remote sensing applications and has demonstrated its effectiveness [109] [110]. For monitor the growth conditions of rice, the ExG at each stage was calculated and the average value in 1 m² was obtained. The ExG index is defined by the following equation.

$$\text{ExG} = 2 * G - R - B$$

3.2.4 Algorithm of K-means cluster

The K-means clustering technique was employed to assess the rice growth conditions. K-means clustering [111] is an unsupervised and straightforward algorithm used to classify data into k clusters (c1, c2, c3, ..., ck), each represented by its centroid. It aims to minimize the squared Euclidean distance between the data points and their respective cluster centroids, enabling the segmentation and classification of the dataset. we used the elbow method [112] to find the optimized number of clusters to be 3, 3, and 2 in class 2, class 3 in 2018 and class 2 in 2019. The key parameter for this algorithm is the number of clusters, denoted as 'k'. Determining the optimal value of 'k' is crucial, as it greatly impacts the performance of K-means clustering. One approach to identifying the optimal value of 'k' is the elbow method. By fitting the model with different 'k' values, a curve can be plotted representing the loss (sum of squared distances) against the number of clusters considered. This curve typically takes the form of an elbow [112]. The point of the elbow on the curve indicates the optimal number of clusters, as the loss does not decrease significantly beyond that point. Analyzing this elbow point helps in determining the suitable number of clusters for the given dataset.

3.2.5 Analysis of rice yield

The procedure of statistical analysis is summarized by the flowchart in figure (3.2). The linear relationships function built in Python was used to understand the relationships between the average VI and rice yield at each sampled point, and then the coefficient of determination (R^2) was obtained. The R^2 for different VIs at different growth stages were acquired and compared with each other. The difference in R^2 showed the regression ability of the VI, and the higher the R^2 , the more precise the results will be.

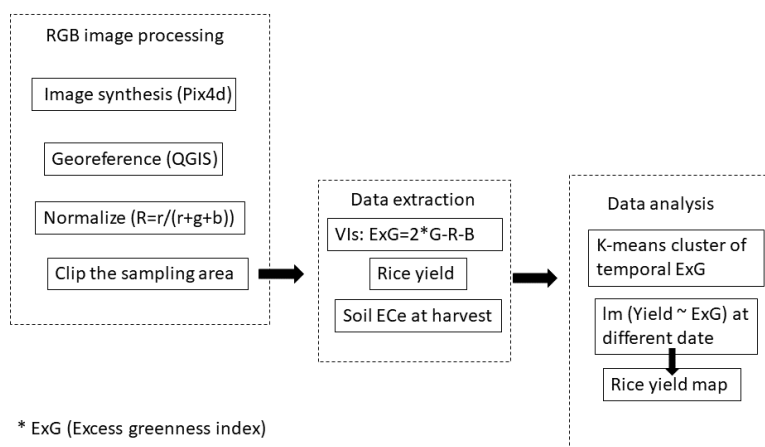


FIGURE 3.2: Experiment methodology and procedure of statistical analysis in this study

3.3 Results

3.3.1 Estimating rice growth based on vegetation index by using UAV RGB images.

In the 2018 class 2 dataset, the ExG values were grouped into three clusters, each cluster has their own characteristics (3.3). In cluster 1, the ExG values remained relatively stable but were lower compared to the other clusters. Cluster 2 demonstrated a correlation with rice growth, showing an increase during the vegetative growth stage from September to October. It reached their peak in mid-October and

Chapter 3. Evaluate rice growth and production in farmer fields under salinity stress by Unmanned Aerial Vehicle (UAV) RGB images in Khon, Kaen, Northeast Thailand.

remained saturated, gradually decreasing before the harvest. On the other hand, cluster 3 displayed a decreasing trend in ExG values towards the harvest. The box plots presented here illustrate the ECE values and rice yield across different clusters (3.4). It appears that the ECE values did not show significant differences among the clusters. However, the rice yield in cluster 2 was relatively higher compared to cluster 1 and cluster 3. Overall, these findings suggest that the ExG values in cluster 2 align with the growth stages of rice, while cluster 1 and cluster 3 exhibit different patterns. The ECE values do not seem to vary significantly across the clusters, but there is a noticeable difference in rice yield, with cluster 2 displaying higher yields compared to the other clusters.

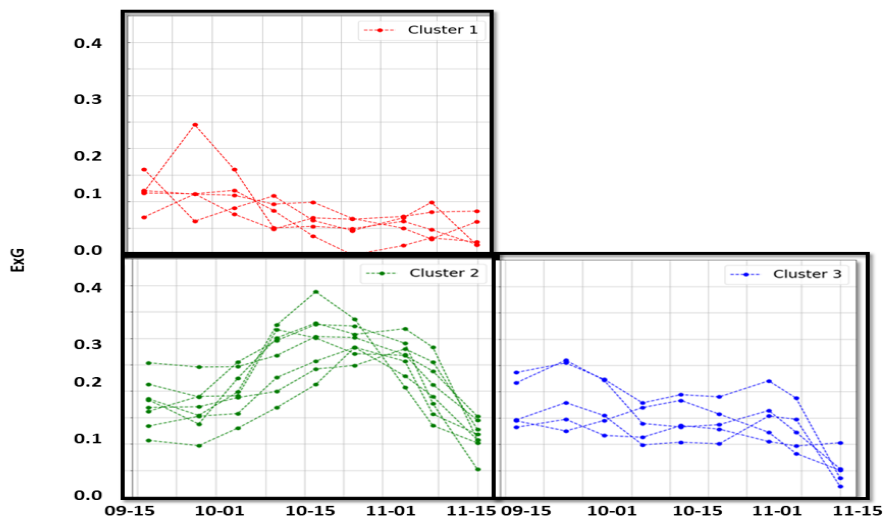
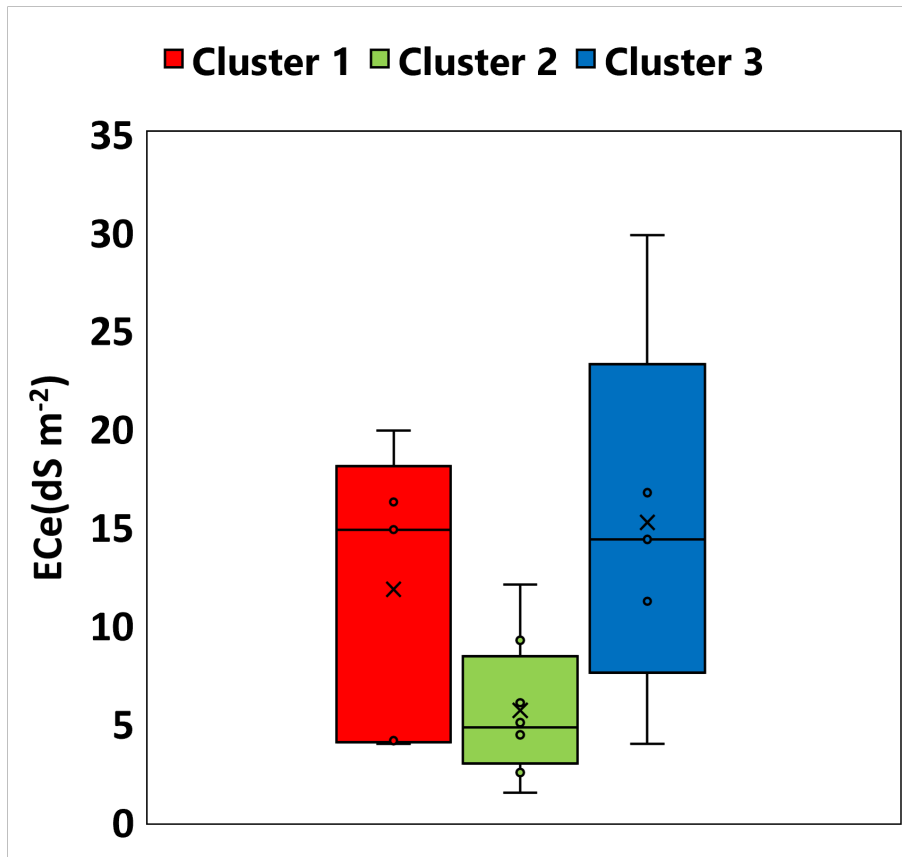
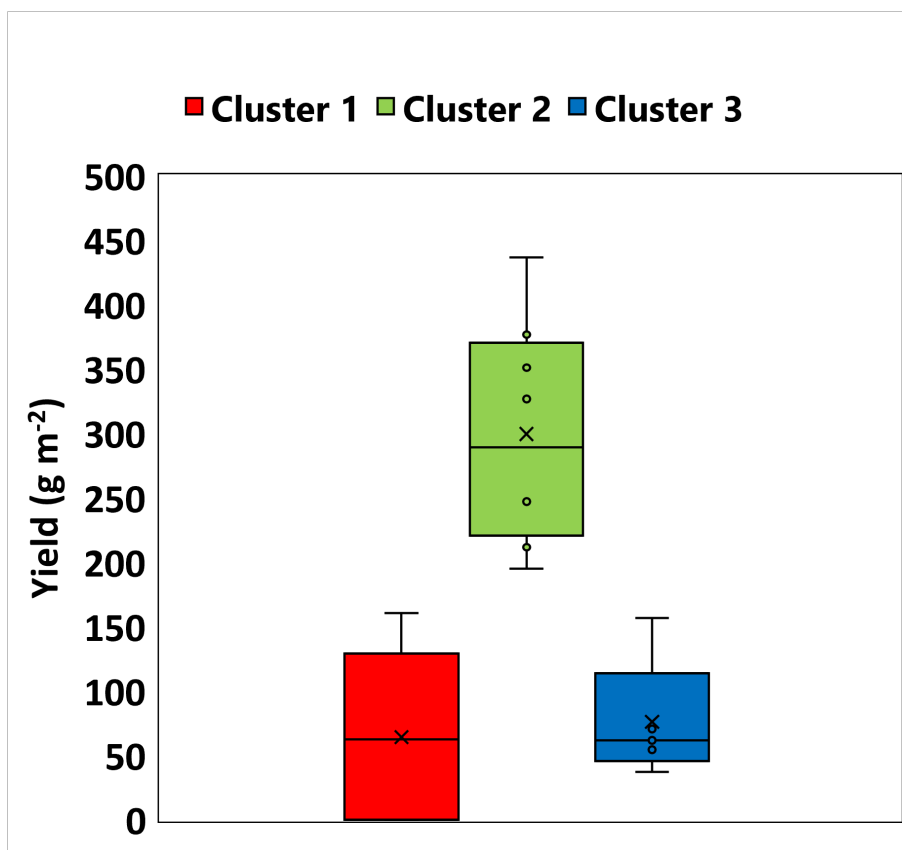


FIGURE 3.3: ExG of sampling points based on characteristic of k-means cluster in class 2 in 2018.



(a)



(b)

FIGURE 3.4: Boxplot of ECe (a) and yield (b) among clusters in class 2 in 2018.

In the 2018 class 3 dataset, the ExG values were also classified into three clusters (3.5). Cluster 1 exhibited relatively lower values compared to cluster 2 and cluster 3, remaining relatively stable around 0. Cluster 2 showed an increasing trend in ExG values leading up to the harvest, with the peak observed at the end of October. Cluster 3 displayed a narrower range of ExG values, ranging from 0 to 0.1. The box plot analysis of ECe did not indicate any significant differences among the clusters (3.6). However, when considering rice yield, it was observed that cluster 2 had higher yields compared to cluster 1 and cluster 3.

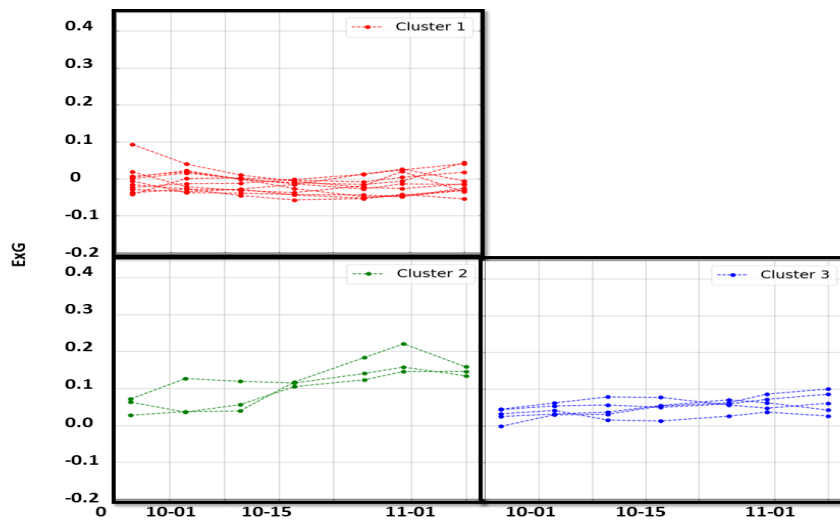
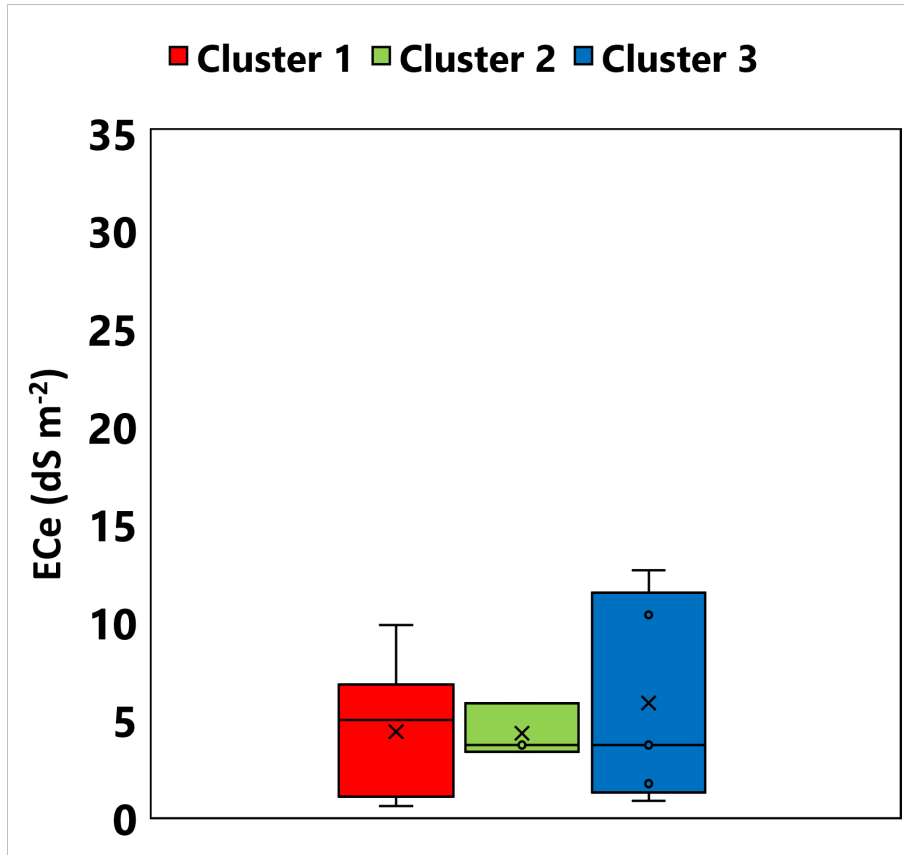
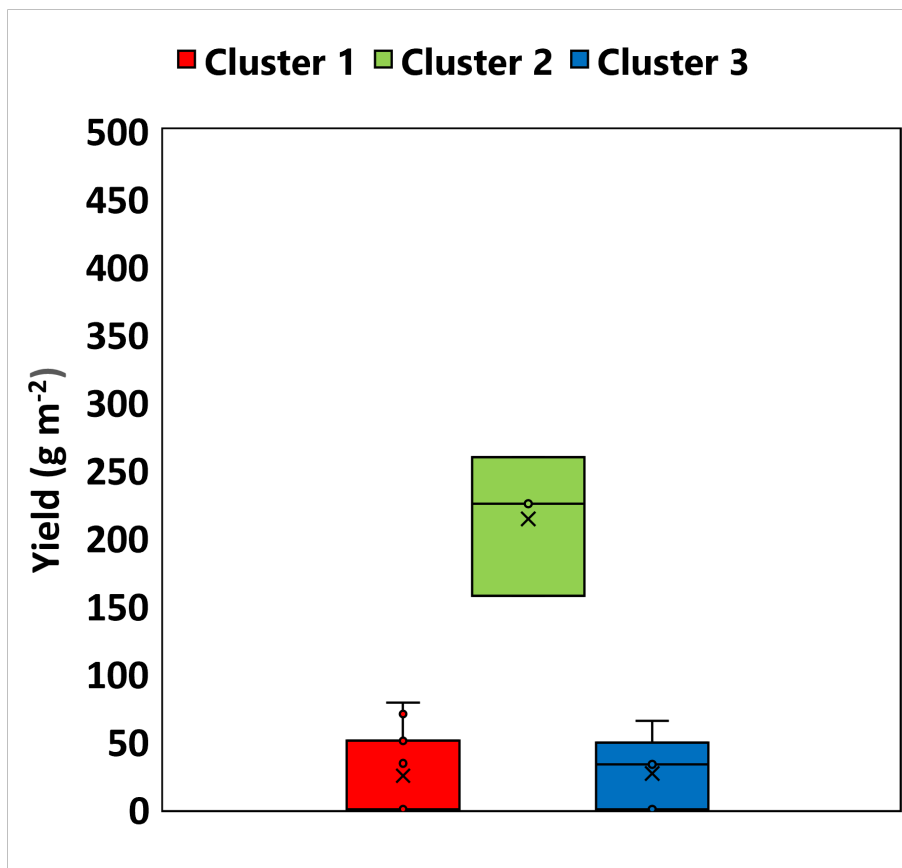


FIGURE 3.5: ExG of sampling points based on characteristic of k-means cluster in class 3 in 2018.



(a)



(b)

FIGURE 3.6: Boxplot of ECe (a) and yield (b) among clusters in class 3 in 2018.

The ExG dataset from class 2 in 2019 can be divided into two clusters (3.7). Both clusters exhibited maximum values in mid-October and gradually decreased leading up to the harvest. The ECe values in cluster 2 were slightly lower than those in cluster 1. Additionally, the rice yield in cluster 2 was higher compared to cluster 1(3.8).

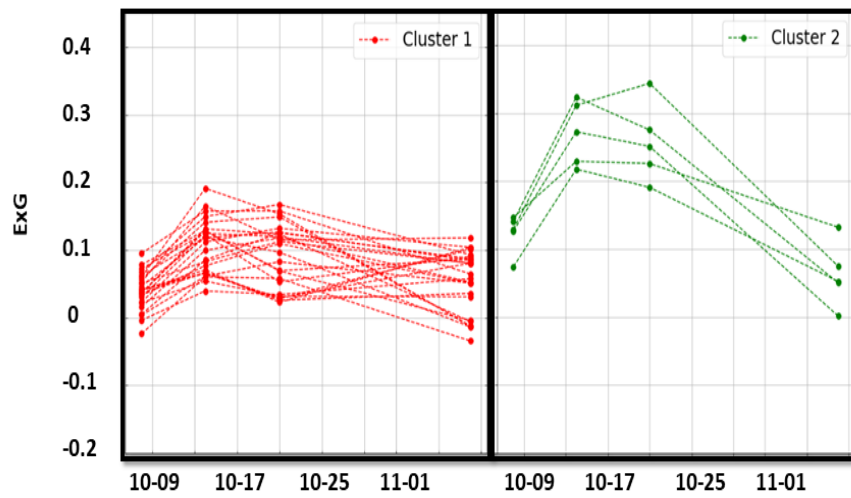
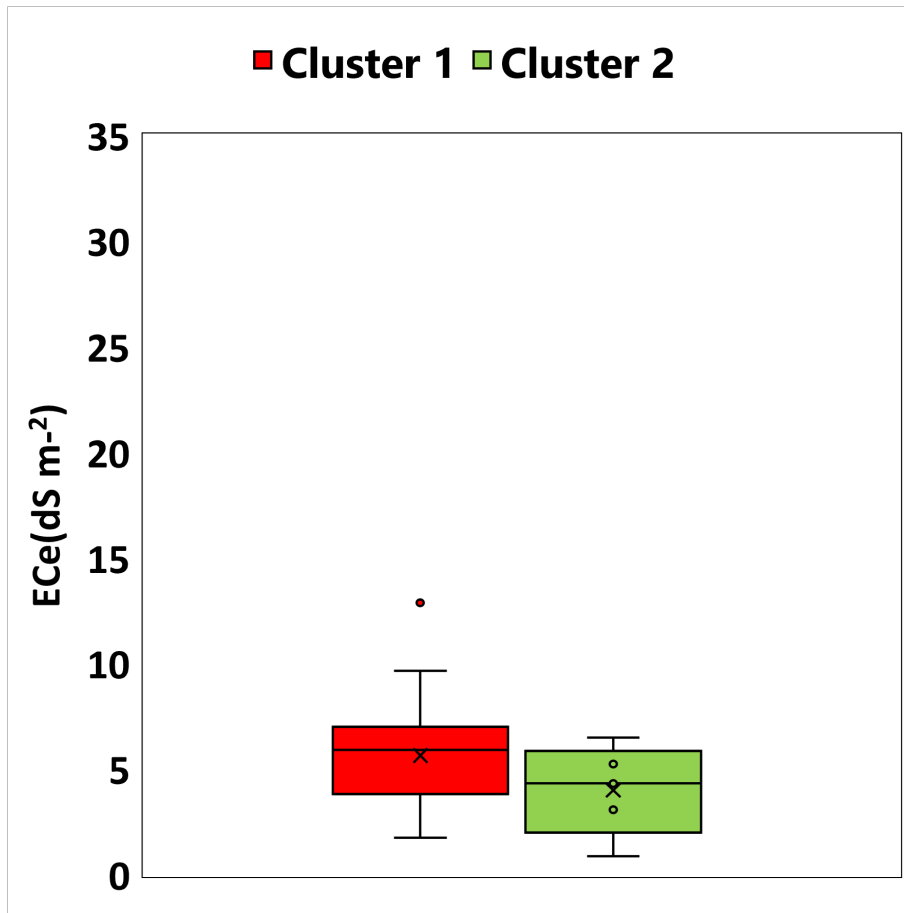
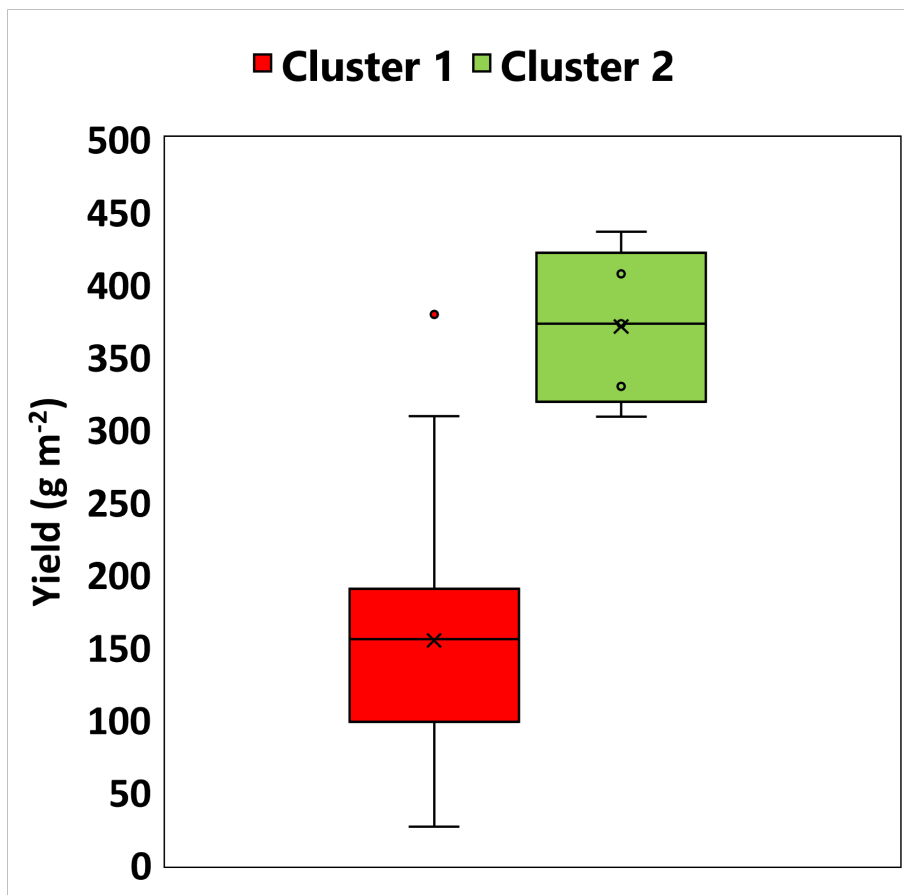


FIGURE 3.7: ExG of sampling points based on characteristic of k-means cluster in class 2 in 2019.



(a)

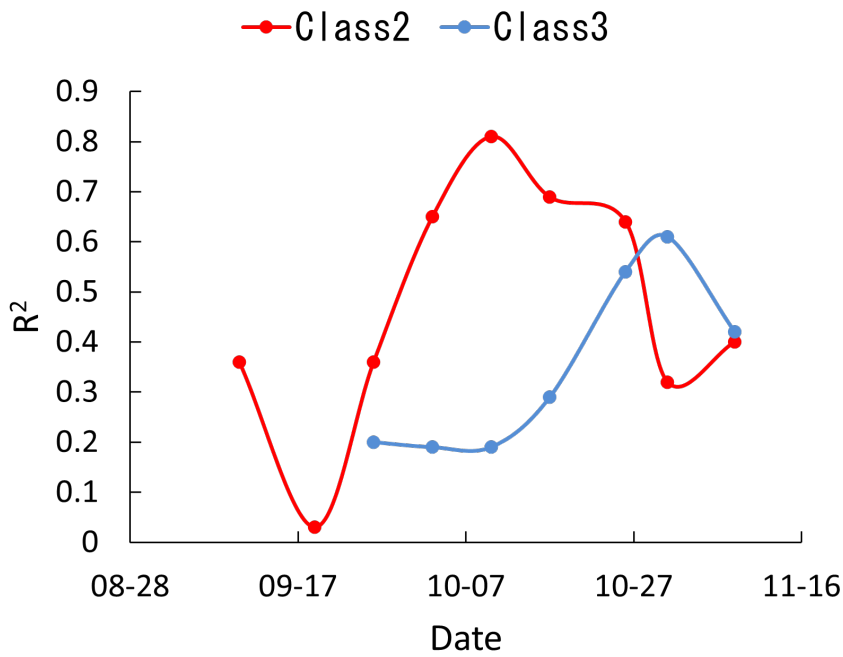


(b)

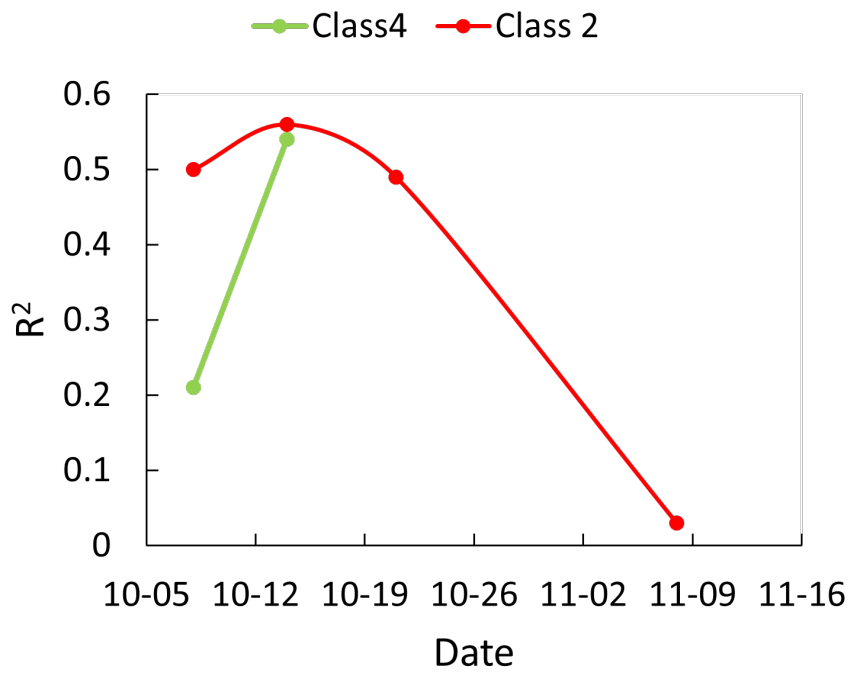
3.3.2 The relationship between rice yield and ExG on different rice growth stage.

The coefficient of determination for the relationship between rice yield and ExG at different stages of rice growth is presented in (Figure 3.9). In the vegetative growth stage of rice, the coefficient of determination (R²) tends to increase. However, it decreases before harvest towards the end of October and the beginning of November. The highest R² values were observed in October, with the peak occurring in mid-October when rice was around the heading and flowering stage for class 2 in both 2018 and 2019. It is important to note that this change in R² was not observed in class 3 in 2018. Instead, in class 3 of 2018, the R² tended to increase towards harvest, with the highest value observed at the end of October.

The figure (3.10) displays the relationship between ExG and yield with the best R² values achieved on 10th October in class 2 in 2018, 31st October in class 3 in 2018, 14th October in class 2 and in class4 in 2019, respectively. These linear regression equations, derived from the analysis, were subsequently utilized to generate a rice yield map in the subsequent analysis.

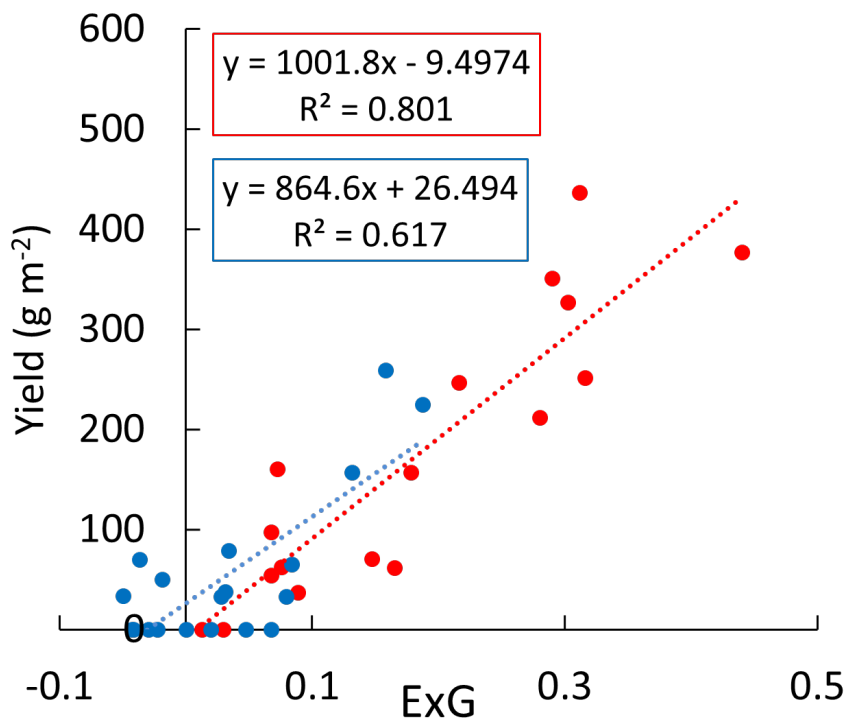


(a)

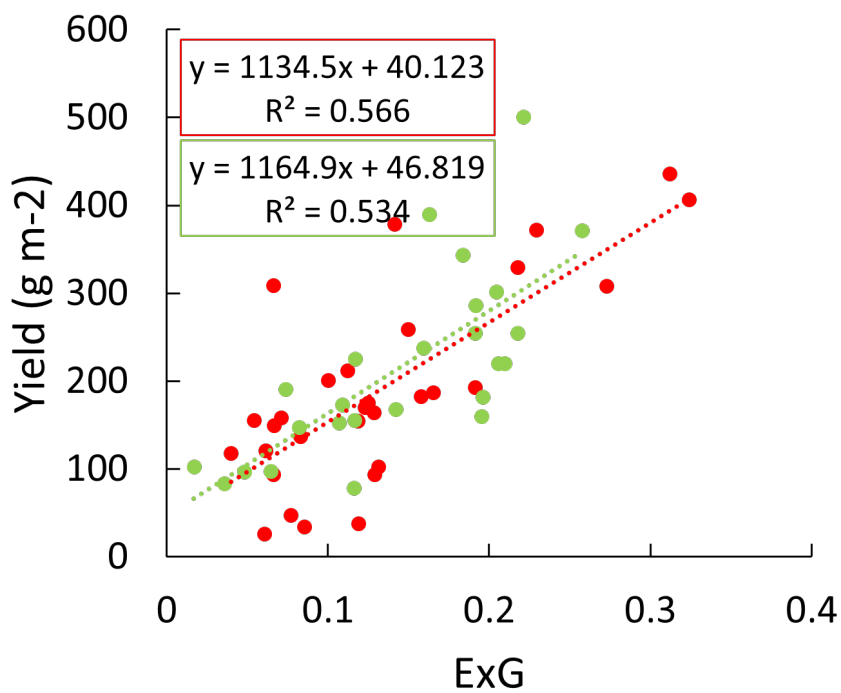


(b)

FIGURE 3.9: The R^2 of the relationship between yield and ExG on different rice growth stage in 2018 (a) and 2019 (b).



(a)



(b)

FIGURE 3.10: The relationship between rice yield and ExG on the best R^2 date in 2018 (a) and 2019 (b).

3.3.3 Rice yield map based on RGB images.

The figure (3.11) illustrated the spatial variation in rice yield. Interestingly, significant differences were observed in rice yield even among nearby paddies. Moreover, within the same paddies, there was also noticeable variation in yield. In class 3, most of rice in paddies were damaged, especially, in the blue rectangle. The rice yield distribution map for the year 2019 reveals that rice yield in class 4 is generally more stable and higher compared to class 2. Notably, the yellow rectangle represents an area where rice yield is consistently low in both 2018 and 2019. This suggests that salinity could be a significant factor contributing to the decline in rice yield at these specific locations.

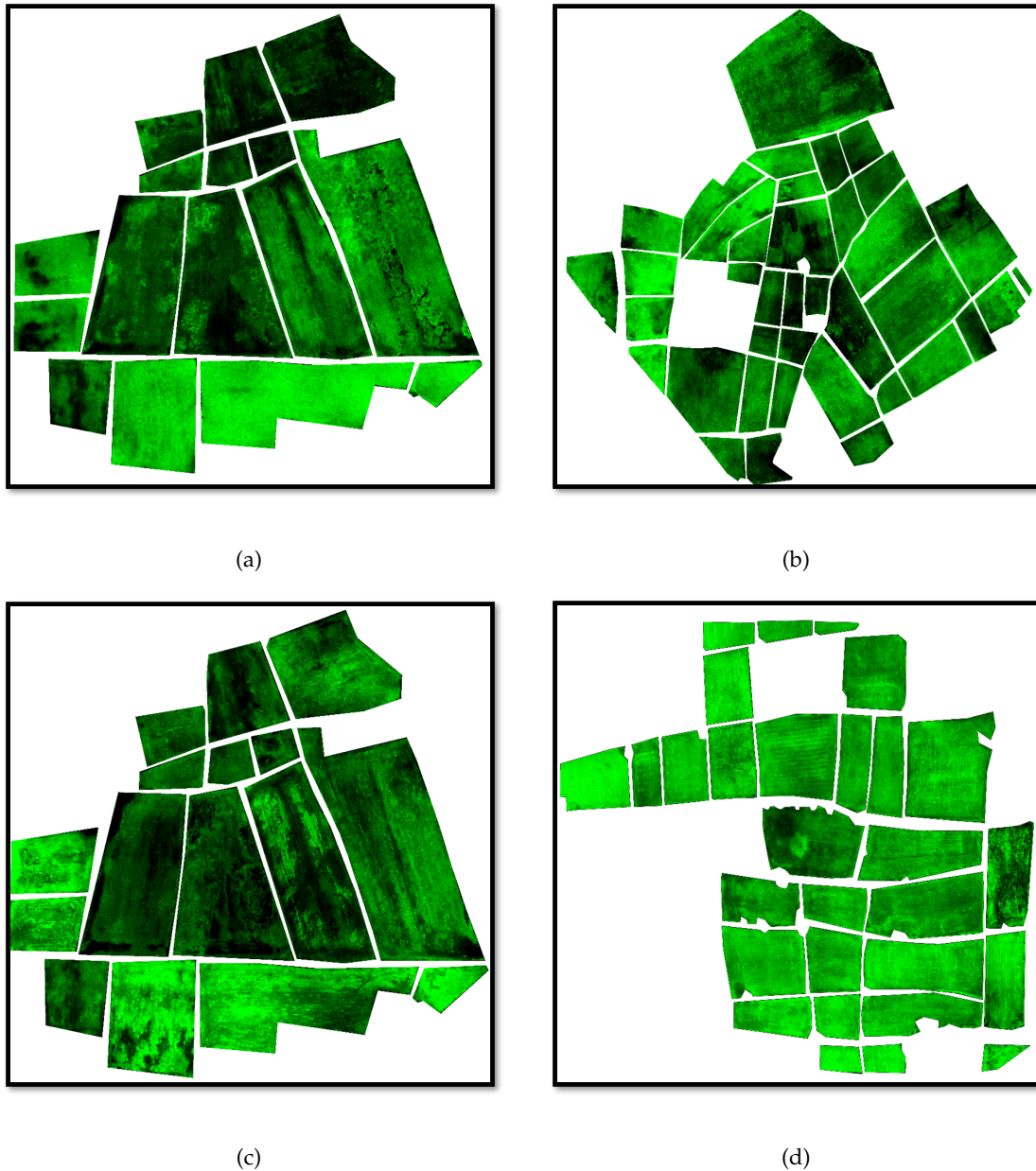


FIGURE 3.11: Rice yield map based on RGB images in class 2 in 2018 (a), in class 3 in 2018 (b), in class 2 in 2019 (c) and class 4 in 2019 (d).

3.4 Discussions

Many previous studies have used UAVs to monitor crop growth indicators, focusing on monitoring a single indicator at a certain stage [113][114]. To test the applicability of using UAV imagery for rice growth detection, commonly used ExG was selected to detect the different rice growth at different locations. The VI (ExG) had great potential in assessing and monitoring the growth of condition of rice, which is agreed

with the previous studies where the VI had been proven to have great potential abilities in agriculture [115] [116]. The ExG from different growth stage were the indicators representing the real-time growth stage condition. Some researchers also used UAV equipped with hyperspectral cameras, multispectral cameras, and lidar [117] [118] [119]. Although such monitoring may reflect the growth status of the vegetation better than using RGB camera, it was not easy to popularize and apply due to its high cost. In contrast, the researchers in this study used RGB images captured by UAVs at different rice growth stages. By calculating corresponding VIs from these images, they successfully estimated rice growth indicators. This approach proved to be straightforward for analysis, applicable to rice growth in the field, cost-effective, and provided rapid and reasonably accurate assessments of rice growth conditions. Consequently, it offered valuable guidance and suggestions for field management decisions. However, using UAV RGB images to monitor rice growth has its limitations, such as being limited to smaller-scale monitoring due to the UAVs' flight time constraints [120]. For broader applications, satellite remote sensing images would be required. However, satellite images have lower spatial resolution compared to UAV images and can be affected by weather changes, making it challenging to achieve precise agricultural guidance at the plot level. Thus, future research should explore the integration of the advantages of both UAV and satellite remote sensing images to effectively monitor crop growth [121] [122].

The application of k-means clustering methods allowed for the grouping of similar rice growth situations into distinct classes, leading to improved precision agriculture practices. In the year 2018, the different rice growth patterns in class 2 and class 3 were successfully detected. Notably, a delay in maximum ExG was observed in class 3 during that year. Surprisingly, rice growth variations were even evident within the same classes. Further analysis of the E_{Ce} values within the different ExG groups revealed that soil salinity did not appear to have a direct correlation with rice growth in 2018. In contrast, based on the author's field investigation in 2018, it was found that water availability emerged as the primary limiting factor for rice growth [123]. Interestingly, the distribution of irrigation practices within class 2 and class 3 resulted in micro variations in rice growth. Notably, comparing rice yield across different ExG groups, higher yields were observed when the changes in ExG aligned

with the healthy rice leaf expansion trend. This trend involved gradual increases in leaf area during the vegetative growth stage, followed by a decrease before harvest due to leaf withering and yellowing [124]. These findings suggest that precise management of water resources and considering the health and growth patterns of rice leaves are critical factors for optimizing rice yield. The k-means clustering approach, combined with the evaluation of ExG and other growth indicators, can offer valuable insights for tailoring agricultural practices and achieving better crop productivity in rice farming.

These years, a lot of researchers are focus on rapidly predict crop yield in real time based on RS data. Many VIs have been proved efficient for predicting crop yield, such as NDVI and EVI2, in grain yield prediction in wheat [125], barley [126], maize [127] and soybean [128]. However, there are few reports describing crop yield prediction based on UAV system, especially, in RGB camera. In this study, the relationships between rice grain yield and the VIs (ExG) from RGB images were tested at different growth stages based on images taken by a UAV. Results showed that ExG of heading and flowering stage had a higher correlation with rice grain yield. This result was consistent with the previous report that the heading and flowering stage could provide higher prediction accuracy when using RS to predict rice yield [129] and [130] also successfully predicted rice yield using reflectance measured at the flowering stage. Thus, the flowering stage may be the best period and the boundary point for the estimation of rice grain yield. The heading and flowering stage around the medium of October has the highest ExG, which can well reflectance the maximum photosynthetic and yield potential [131]. [132] used the maximum VIs to estimate wheat yield. At the early rice growth stages, rice paddies were merged by stand water, water can affect ExG value easily. At the maximum VIs stages, VIs can be easily saturated due to the high level of vegetation coverage [133]. In the later growth stages, the appearance of the rice panicle, the increase in yellow leaves and leaves withering enhances the difficulty of yield prediction.

The rice yield map based on RGB images exhibited inconsistencies across classes and years, which did not align with the findings of the field investigation in chapter 2. The rice yield map demonstrated variations in yield among different classes and even within the same class. These results suggest that assessing rice yield through

field investigation becomes more challenging due to the significant yield variations, even when locations are in close proximity. Interestingly, the field investigation [123] indicated that rice yield in class 3 was significantly lower than in class 2 in 2018. However, this study observed a larger-scale damage to rice yield in class 2 compared to class 3. Further analysis of the rice yield map in class 2 for the years 2018 and 2019, which experienced different rainfall patterns, revealed the presence of similar lower-yield locations. This finding suggests that the reduced rice yield in class 2 might be attributed to salinity-related issues. These results emphasize the complexity of understanding rice yield variations and the importance of considering multiple factors such as salinity, rainfall, and local conditions when interpreting rice yield maps. The combination of remote sensing data and field investigation can provide a more comprehensive understanding of the factors influencing rice yield, helping farmers and researchers make informed decisions to improve agricultural practices and mitigate yield losses.

3.4.1 Conclusion

UAVs have become a new platform for acquiring high spatiotemporal resolution images used for precision agriculture. The multi-temporal VIs were explored for rice growth detection and the single stage VI was explored for rice grain yield estimation based on RGB images from UAV. This study has demonstrated that RGB images acquired are reliable for rice growth and grain yield estimation.

The heading and flowering stage was proved as the best growth stage for grain yield estimation with VI from a single stage for RGB images. However, the yield estimation models and method should be further examined with more datasets. In addition, some new technology such as machine learning method and some yield-related agronomic parameters such as LAI and crop growth period can be further analyzed and integrated with UAV datasets to improve rice grain yield prediction accuracy.

Chapter 4

Yearly change in severely damaged areas in paddy fields in khon kaen,northeast Thailand.

4.1 Introduction

Soil salinity, which affects crop production due to the accumulation of toxic ions and the inhibition of water and nutrient absorption [134], is considered a serious global problem in terms of food security [135]. Northeast Thailand is a severely salt-affected region; more than 3.3 million ha are estimated to be salt-affected in the area [136]. The soil salinity is derived from underground salt rock in Northeast Thailand [137]. Accordingly, the groundwater has a considerable effect on salinity, further complicating the situation [138][139]. Some studies have reported the expansion of salt-affected areas [140], but the details of these expansions are still unknown.

Rice is a major agricultural product in Northeast Thailand. Rice paddy fields occupy more than half of the agricultural land, but their production levels are both low and unstable [141][142]. Since irrigation facilities have not yet been developed, most rice production is conducted under rainfed conditions. Precipitation shows yearly and spatially large variations, frequently causing drought and flooding. Compared with drought and flooding, the salinity problem for rice production is rather localized [143]. However, since some farmers are starting to abandon their paddy fields

due to severe salinity, the problem has become one of the major issues affecting rice production in Northeast Thailand [144] [145].

Based on the situation described above, we conducted field investigations to evaluate salinity conditions in relation to rice production in Ban Phai district, Khon Kaen province in Northeast Thailand, which is one of the most severely salt-affected regions. One accompanying papers in this special issue analyzed soil salt accumulation by simulating soil water movement [139]. We also analyzed spectral reflectance of salinity affected fields to evaluate salinity conditions at a regional scale with satellite remote sensing [146]. This report focused on yearly changes in rice production and salinity conditions. In particular, the yearly movement of severely salt-damaged areas in paddy fields was evaluated on the basis of RGB images taken by unmanned aerial vehicles (UAVs).

4.2 Materials and methods

4.2.1 Study area

The investigation site Figure(2.1) was located in Ban Phai district, Khon Kaen province in Northeast Thailand. The area is classified as having a tropical savanna climate and has 2 seasons (a rainy and a dry season). The rainy season starts in May and ends in October. Precipitation data were collected from the meteorological station in Ban Phai, Meteorological Department, Thailand. Since irrigation facilities have not been developed in the study region, rice was planted only in the rainy season under rain-fed conditions. The soil salinity level was officially classified into 5 classes (class 1 corresponds to very severely salt-affected soils; class 5 corresponds to non-salt-affected soils) by the Land Development Department, Thailand (Wichaidit, 1995; Katawatin and Sukchan, 2012). The investigation site was classified as class 2, comprising severely salt-affected soils. Some farmers continued to plant rice in the study region, but others had abandoned their paddy fields due to the severe salinity conditions.

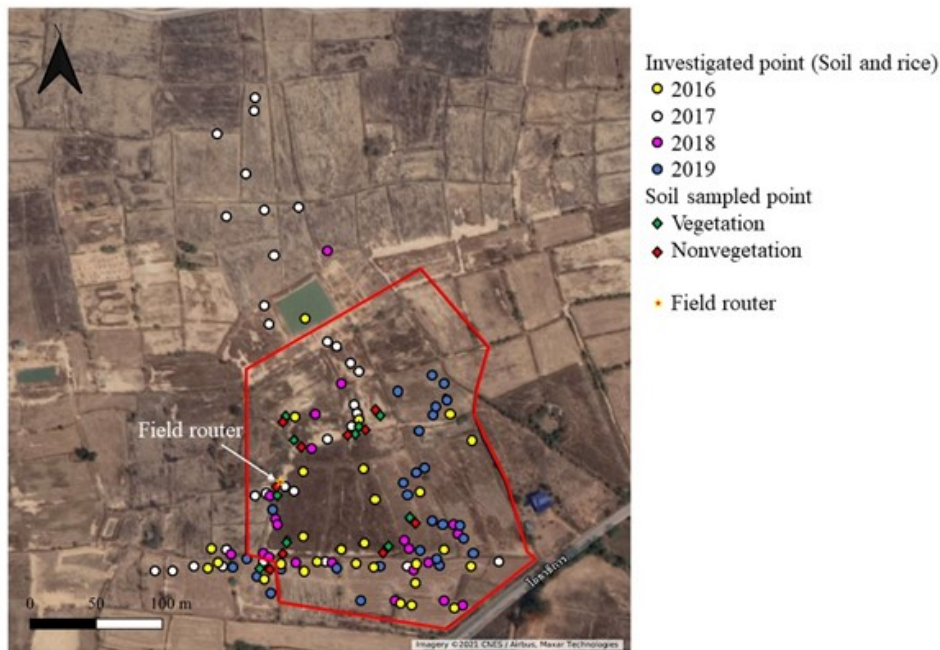


FIGURE 4.1: The investigated fields on Google Maps. Circles show the investigated points for soil EC and rice yield in Figure 3 and 4, respectively. Rhombuses show the soil sampled points to support non-vegetated/vegetated analysis in Figure 5 and 6. EC and depth of ground water were measured with the field router.

4.2.2 Measurement

Yield measurements were conducted at 29, 34, 19 and 30 points in rice-planted paddy fields in 2016, 2017, 2018 and 2019, respectively (2.1). Although the harvested points varied from year to year because some fields were not planted based on the farmers' decision, the points were selected to represent the rice planted paddy fields in the area. Rice plants were harvested in a 1 m² circle at each point on November 12, 2016, November 5, 2017, November 6, 2018, and November 8, 2019. The grain was threshed, and its weight was calibrated with its moisture content, which was measured with a grain moisture meter (CD-6E, Shizuoka Seiki). Five hundred ml of plow layer soils were collected uniformly from the surface to 12 cm depth at the 34, 19 and 30 harvested points in 2017, 2018 and 2019, respectively, at the same time that the rice plants were harvested. The soil samples were ground and sieved in 2-mm sieves after being air dried. The soil EC (soil:water = 1:5) was measured using an EC meter (FiveEasyTM Plus EC meter FEP 30, Mettler Toledo).

4.2.3 Analysis

RGB images were collected at the rice harvest, just after the rainy season ended, by UAVs: a 3DR Soloon November 12, 2016, a DJI Phantom 4 on November 6, 2018, and by a DJI Mavic pro on November 8, 2019. We tried to take RGB images on November 5 and 6, 2017, but failed due to strong winds. The flight height was 50 m at approximately 2 cm/pixel resolution. The images, synthesized by Photo-scan Professional (Agisoft), were georeferenced by QGIS based on Google Maps. A 4.3-ha area, which was common to the images in 2016, 2018 and 2019, was analyzed to evaluate the non-vegetated/vegetated areas with a support vector machine (SVM) in scikit-learn for Python [147]. One hundred buffers for non-vegetation and 100 buffers for vegetation were selected in each image. The representative non-vegetated/vegetated area was determined with observation and recorded by GPS receiver (eTrex 20x, Garmin). The non-vegetated/vegetated buffers were selected in each representative area with checking the RGB image. The buffer was set at a 1-m × 1-m square to obtain the minima, maxima, means and medians of R, G and B. Seventy five percent of buffers were used for training, and the rest were used for validation. The image was divided with 1-m × 1-m meshes and was then subjected to supervised classification with SVM. The accuracies for the validation buffers were 0.88, 0.98 and 0.98 in 2016, 2018 and 2019, respectively. Soils were sampled uniformly from the surface to 12 cm depth at 10 non-vegetated points and at 10 adjacent vegetated points on October 9, 2019 (2.1). The EC (soil:water = 1:5) for the sampled soil was measured using the same method for soils at the rice harvesting points.

4.2.4 algorithm of SVM

Support Vector Machine (SVM) is a supervised, non-parametric statistical learning technique initially proposed by Vapnik in 1979 [148]. SVM utilizes a set of labeled data points and employs a training algorithm to identify a hyperplane that effectively segregates the dataset into distinct predefined classes, aligning with the provided training examples. SVM has demonstrated its efficacy in various applications, particularly excelling in scenarios characterized by limited data samples, nonlinearity, and high-dimensional pattern recognition [149].The primary objective of SVM

is to determine a decision surface, established by specific points within the training dataset, known as support vectors. These support vectors play a pivotal role in the SVM's classification process, ensuring that all data points within the same class are situated on one side of the decision surface. Moreover, SVM strives to maximize the margin, which is the minimum distance between the decision surface and any data point from either of the two distinct classes. This margin optimization is a fundamental aspect of SVM's classification prowess.

Cohen's kappa index was employed to estimate the accuracy of SVM classification [150]. It was performed using information about several statistical evaluation criteria such as true positive (TP), false positive (FP), true negative (TN), and false negative (FN) [151], the kappa coefficient (K) is gained by measuring the ratio of observed agreements (Pobs) and expected agreements (Pexp) as follows:

$$K = (P_{obs} - P_{exp}) / (1 - P_{exp})$$

Where, $P_{obs} = (TP+TN)$ represents the proportion of pixels that are correctly classified as non-vegetation or vegetation area. $P_{exp} = (TP+FN)(TP+FP) + (FP+TN)(FN+TN)$ is the proportion of pixels for which agreement is expected by chance [150]. [152] stated that Cohen's kappa index is closer to 1 means the model and the reality is more agreement.

4.3 Results and discussion

Precipitation varied from year to year(4.2) . Rainfall was abundant in 2017 but quite limited in 2018 and 2019. Although the amounts were similar between 2018 and 2019, the patterns were quite different: the precipitation level was high from April to July in 2018 but high in May and August to September in 2019. In 2019, some paddy fields near the investigation area were delayed for rice planting due to inadequate rainfall in June and July and suffered from flooding due to heavy rainfall in August and September. The precipitation level from August to October, which is

the most important duration for rice production at the site, was 269 mm in 2018, which was approximately half of the average (515 mm).

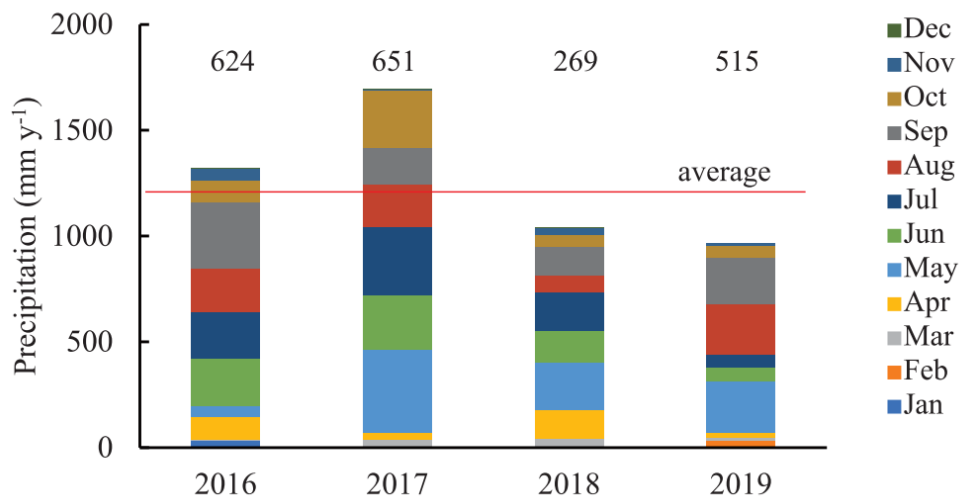


FIGURE 4.2: Precipitation from 2016 to 2019 in Banphai. The numbers on the bars indicate precipitation amount between August and October.

The soil EC in rice-planted paddy fields varied from year to year and seemed to be associated with precipitation, especially from August to October(4.3). Although the lowest ranges of soil EC were quite similar from year to year, the highest values differed extensively.

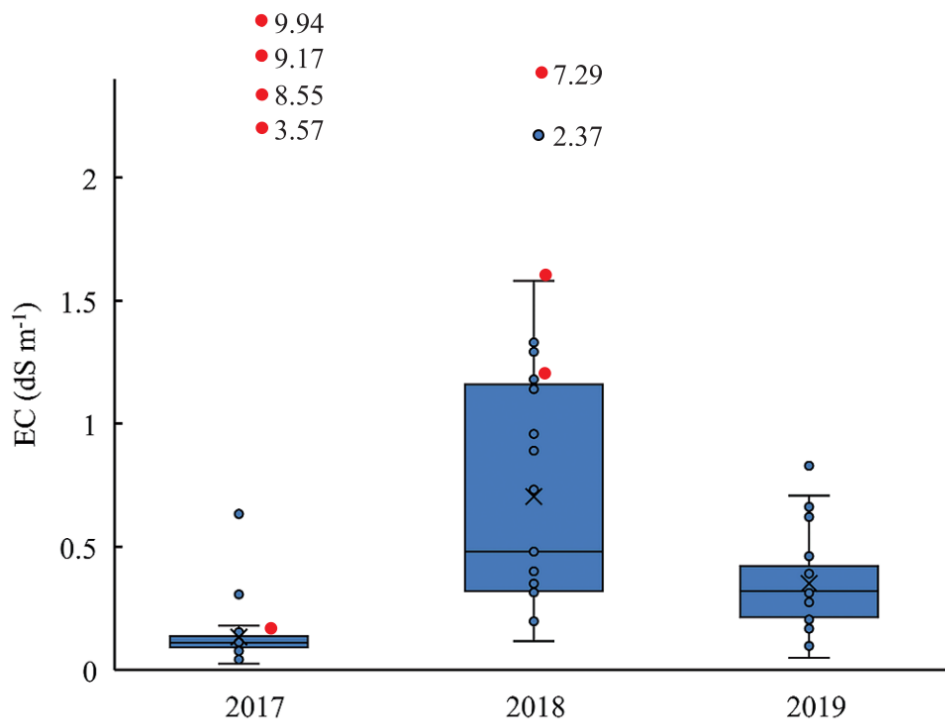


FIGURE 4.3: Box plot of soil EC (1:5,soil:water) of investigated paddy fields from 2017 to 2019. The number of samples was 34,19 and 30 in 2017 ,2018 and 2019,respectively. The number to right of each symbols the EC,which exceeded 2.0 dS m⁻¹. Red symbols indicate the EC where the rice yield was 0 g m⁻².

The rice yield showed large variation and many fields showed quite low yield (4.4). For example, one fourth of the fields recorded less than 54 g m⁻² of yield in 2018. The average rice yield seemed to be associated with precipitation. Higher rice yield was expected due to higher precipitation in 2017. However, the abundant rainfall caused farmers to plant paddy rice even in salinity fields (4.3), which decreased the average yield. The abundant rainfall sometimes caused lodging due to excess stem growth, which also decreased the average yield in 2017. The yearly variation in rice yield was smaller than those in precipitation and soil EC. The effects of precipitation and then soil EC on rice production were probably alleviated by surface water. Our preliminary analysis suggested that the classification of soil EC_e (i.e. the EC of the soil saturation extract) clearly categorized the effect of salinity on rice production. A detailed analysis of the relationship between soil salinity and rice production will be described in another report.

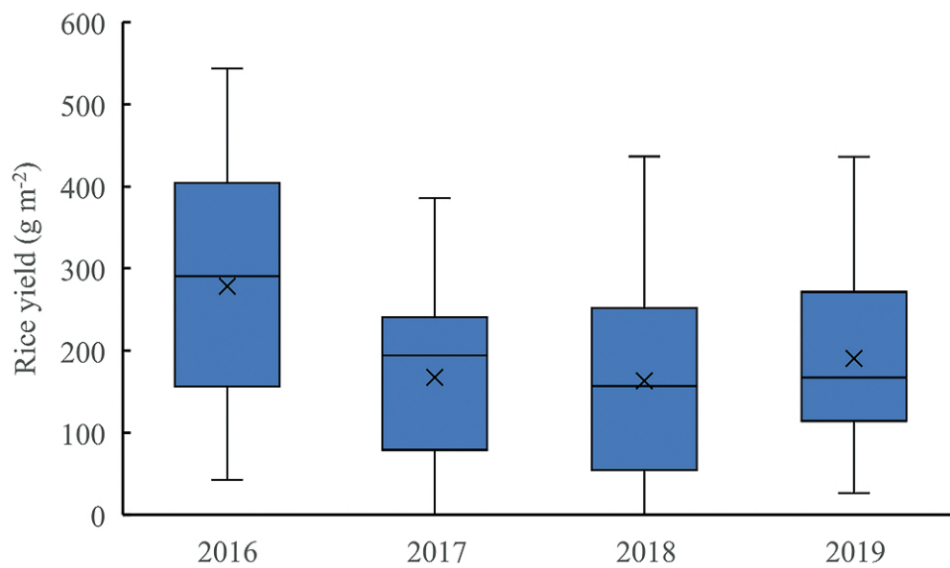


FIGURE 4.4: Box plot of rice yield of investigated paddy fields from 2016 to 2019. The number of samples was 29,34,19 and 30 in 2016,2017,2018 and 2019,respectively.

The soil EC in the non-vegetated area ($2.6 \pm 3.5 \text{ dS m}^{-1}$) was significantly higher than that in the vegetated area ($0.16 \pm 0.11 \text{ dS m}^{-1}$). Salt crusts were clearly observed in RGB images in 2018 and 2019, although the images were taken just at the beginning of the dry season (white areas in 4.5. The scarce precipitation in October in both years might enhance the appearance of salt crusts earlier in the season. Non-vegetated areas occupied 11.4%, 14.6% and 10.0% of the analyzed area in 2016, 2018 and 2019, respectively. No clear tendency towards expansion of the non-vegetated areas was observed. The non-vegetated areas also did not show clear associations with precipitation or soil EC in rice-planted fields. Some non-vegetated areas expanded from 2016 to 2019, while others were reduced (4.7). The reduction of non-vegetated areas may suggest that the soil EC was partly alleviated by non-rice planting. The localized differences in the trend of non-vegetated areas were likely affected by groundwater. EC of ground water in the area was high and stable ($44.8 \pm 1.2 \text{ dS m}^{-1}$ from July 16, 2017, to October 6, 2018; data retrieved from [139]) and shallow ($-46 \pm 8 \text{ cm}$, from August 1 to October 6, 2017; $-196 \pm 9 \text{ cm}$ from February 1 to April 30, 2018; $-75 \pm 10 \text{ cm}$ from August 1 to October 6, 2018), being the major resource of salinity.

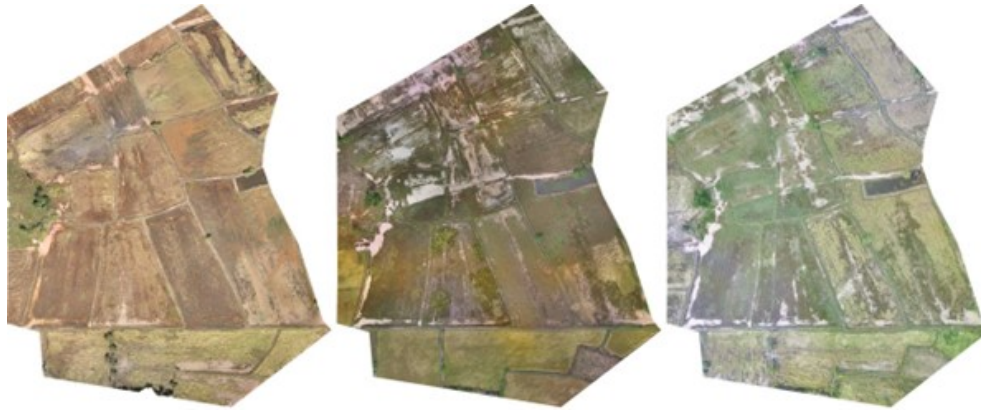


FIGURE 4.5: RGB images for the investigated areas at rice harvest in 2016,2018 and 2019.

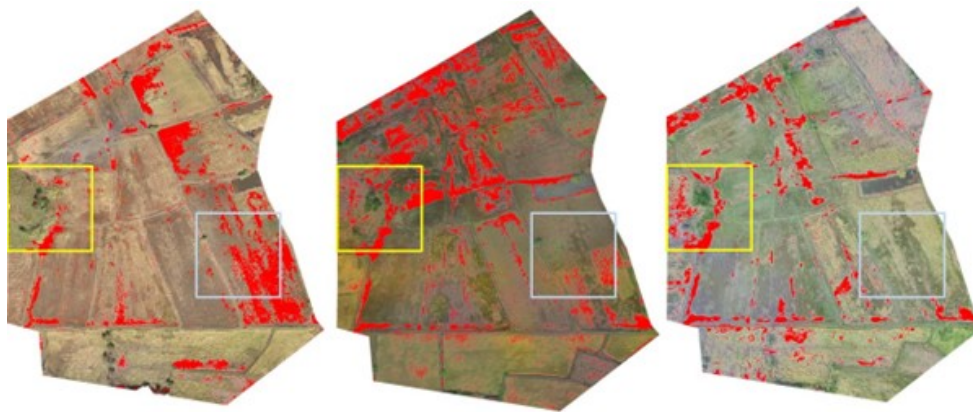


FIGURE 4.6: Non-vegetated/vegetated classification for the investigated areas at rice harvest in 2016, 2018 and 2019. Red areas are classified as non-vegetated areas. Yellow and light blue rectangles are areas shown in Figure 7.

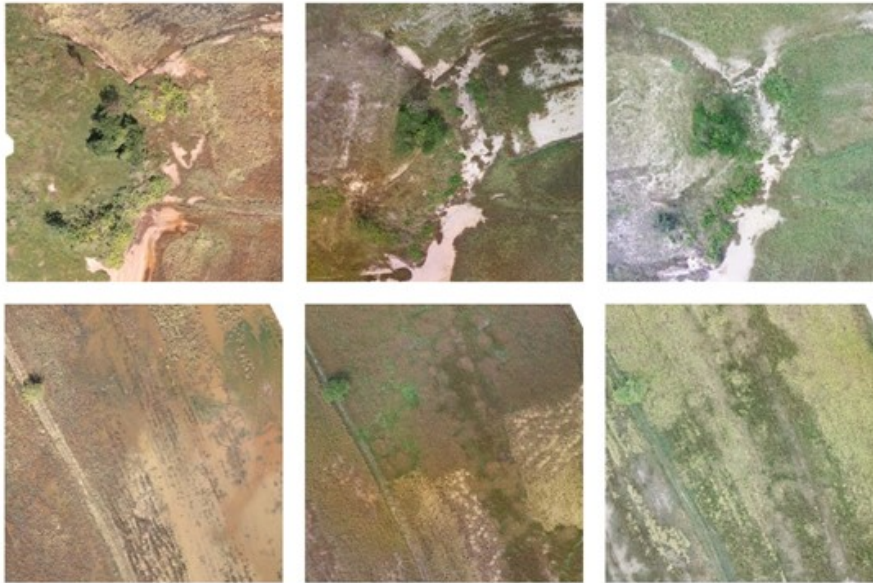


FIGURE 4.7: Changes in vegetation in RGB images in 2016,2018 and 2019 representative areas indicated in Figure 6 (above:yellow rectangle;below:light blue rectangle).

Some studies evaluated salinity-affected areas by utilizing satellite data [153]. The utilization of satellites is quite effective for wider regions, especially for evaluating large and severe salinity-affected areas, such as class1 areas. However, this study showed that quite small pieces of non-vegetated area changed from year to year, suggesting that the threshold of whether a plant can or cannot grow fluctuates locally and yearly. Accordingly, quite a small change that could be evaluated by UAV may be important for evaluating salinity levels in terms of rice production. The authors tested satellite data to directly evaluate soil EC_e, which is quite important for evaluating the effects of salinity on crop production [154]. The combination of soil chemical properties based on satellites with vegetation evaluations based on UAVs would be an effective tool to evaluate the effects of salinity on crop production in wider regions. [139] assessed the climate change impact of soil salt accumulation by simulating soil water content and predicted that soil EC_e would increase in the future. Since this study did not suggest an increasing trend in soil EC or non-vegetated areas, monitoring for longer durations would be necessary. Since the trends of non-vegetated areas differed spatially, the evaluation of groundwater movement is essential for predicting salinity levels at each location. The observation that some areas had vegetation following a lack of vegetation imply that salinity

levels can be alleviated by controlling groundwater, such as through reforestation [155].

4.4 Conclusion

This study conducted field investigation to reveal present conditions in severely salt-affected paddy field areas where some farmers had abandoned their paddy fields due to the severe salinity. The variation in precipitation may be one of the major factors affecting salinity conditions. However, while soil EC in the rice planted fields apparently varied with precipitation, the effects on rice yields were not so obvious. Standing water provably alleviated salinity damage.

Since some fields produced quite low yields, an increase in the abandonment of fields is anticipated in the future. Analysis of non-vegetated/vegetated areas were conducted to evaluate severe salt-damaged areas and to forecast the future availability of areas for rice cultivation. However, increases in non-vegetated area were not explicitly observed because some areas changed from non-vegetated to vegetated. The increase or decrease in non-vegetated area geographically varied, suggesting that groundwater is another factor affecting salinity conditions. Further investigation is recommended to reveal the dynamics of salinity conditions and to contribute to the improvements in rice production.

Chapter 5

General

5.1 General discussion

This study assessed soil salinity during the rainy season based on the EC_e value. The findings revealed that the soil's salinity condition during this period did not align with the salt-affected classifications provided by local institutions in Thailand. This observation echoed previous research [156], which highlighted significant variations in salinity levels between dry and wet conditions, attributed to substantial salt content in the subsurface soil solution and water dissolution. Within the study area categorized as classes 2 to 4 by LDD, soil salinity displayed intricate patterns during the unusually low rainfall year of 2018. Notably, salinity conditions in the severely salt-affected class 2 area were significantly higher than those in the slightly salt-affected class 3 area, consistent with LDD's salt-affected classification. In class 2, EC_e values ranged from 2 to 13 dS m⁻¹, whereas in class 3, they ranged from 0.5 to 5 dS m⁻¹. Interestingly, abundant rainfall had a leveling effect on salinity conditions, with no significant differences among the classes. In class 4, the EC_e value was higher than that in the severely salt-affected class 2 area. This outcome may be attributed to saline water irrigation in the rice paddies of class 4 in 2019 [patcharapreecha1989studie]. As a result, given our discovery that the EC_e value in non-vegetated areas is significantly higher than in vegetated areas, in line with prior research indicating that salinity conditions can be indirectly detected through vegetation growth [157], we made the assume that non-vegetated areas represent severely salt-affected zones, while vegetated areas are relatively less affected by salt. In this study, we employed

a machine learning method known as Support Vector Machine (SVM) to distinguish between vegetation and non-vegetation areas using RGB images collected by UAVs. This approach offers an economical and swift means of assessing salinity conditions within small, localized regions. Analyzing the changes in non-vegetated areas over time, we observed that there was no consistent expansion trend in salinity over the years, contrary to findings in a previous study [158]. Therefore, it appears imperative to conduct longer-term monitoring. In northeastern Thailand, the average farm size tends to be relatively small, often comprising several smaller subunits for various purposes. Although numerous researchers have attempted to create salinity maps, their assessments have typically focused on visualizing regional-scale spatial variations in salinity. Such an approach falls short in terms of formulating effective management plans for these small, cultivated fields. Given the scarcity of salinity distribution maps specific to small farms during the rainy season [159], our study represents a fundamental step toward gaining a better understanding of the variability in soil ECe. Subsequently, it paves the way for the development of strategies to manage salt-affected soils in precision agriculture, particularly in class 2, where we observed a wide range of salinity levels.

The adverse effects of salinity on rice yield have led farmers to consider abandoning rice cultivation [160]. However, our investigation has revealed that the negative impact of salinity is not as severe as initially perceived from our images. Our findings indicate that rice yield was only reduced in class 3 during the year 2018, which was characterized by very low soil moisture content and relatively low salinity levels. Interestingly, we observed that in some instances, higher rice yields were achieved even under conditions of elevated salinity, suggesting that drought may be the primary limiting factor for rice yield in our study area. This observation aligns with a previous study by Jongdee [161], which reported yield losses ranging from 55% to 8% due to drought in different locations in northeast Thailand. Additionally, [162] documented an overall 56% reduction in rice production during drought years in the same region. Although we did not identify a significant linear relationship between salinity and rice yield, it is evident that rice yield is adversely affected when salinity levels are quite high. Furthermore, there is a tendency for rice yield to decrease with increasing salinity levels. [163] similarly noted that approximately

20% of rice yield reduction was attributable to salinity, while a substantial 87% reduction was linked to drought. Given our discovery that salinity conditions can be alleviated by standing water during abundant rainfall years, effective water management is critically important for rice cultivation, especially in saline paddies. Furthermore, the use of on-farm resources such as cow manure, compost, and green manure represents environmentally sensitive approaches to mitigating soil salinity. Some researchers have also proposed raising the height of paddy borders as an efficient strategy for enhancing rice yield under saline conditions, as this enables the continuous submergence of rice paddies through rainwater capture [164].

The intricate nature of the paddies presented a formidable challenge when it came to precisely estimating rice yield and assessing salinity conditions. Nevertheless, the application of UAV technology has proven to be a powerful tool in surmounting this challenge. In our study, we harnessed this technology to great effect. By analyzing the vegetation index derived from RGB images, we uncovered a remarkably strong and significant linear relationship with rice yield, particularly during the crucial heading and flowering stages of growth. This revelation suggests that rice yield can be accurately estimated well before the actual harvest, a development of considerable importance for agricultural planning and management.

5.2 General conclusion

This study has provided valuable insights into the dynamic interplay between soil salinity, rice yield and the application of UAV in northeast Thailand. We began by investing soil salinity during rainy season, assessed through the E_{Ce} value, and found that it was not always similar with salt-affected classification by LDD. Climate factor especially rainfall should be considered when we classify soil salinity condition. Moreover, we used vegetation growth as an indirect indicator of salinity conditions with SVM method and RGB images collected by UAVs. This cost-effective method allowed us to assess salinity in small farm. Finally, we investigated rice yield limitation factors in study area, and proved the relationship between vegetation index from UAV RGB images and rice yield, allowing for accurate preharvest yield estimation—an invaluable contribution to agricultural planning and management.

References

- [1] Manzoor Qadir et al. "Economics of salt-induced land degradation and restoration". In: *Natural resources forum*. Vol. 38. 4. Wiley Online Library. 2014, pp. 282–295.
- [2] Konstantin Ivushkin et al. "Global mapping of soil salinity change". English. In: *Remote Sensing of Environment* 231 (Sept. 2019). ISSN: 0034-4257.
- [3] Yan Li et al. "Potential and actual impacts of deforestation and afforestation on land surface temperature". In: *Journal of Geophysical Research: Atmospheres* 121.24 (2016), pp. 14–372.
- [4] Rameesha Abbas et al. "Halotolerant PGPR: A hope for cultivation of saline soils". In: *Journal of King Saud University-Science* 31.4 (2019), pp. 1195–1201.
- [5] Amirhossein Hassani, Adisa Azapagic, and Nima Shokri. "Global predictions of primary soil salinization under changing climate in the 21st century". In: *Nature communications* 12.1 (2021), p. 6663.
- [6] IN Daliakopoulos et al. "The threat of soil salinity: A European scale review". In: *Science of the total environment* 573 (2016), pp. 727–739.
- [7] Jan W Hopmans et al. "Critical knowledge gaps and research priorities in global soil salinity". In: *Advances in agronomy* 169 (2021), pp. 1–191.
- [8] Nyle C Brady. "The Nature and Properties of Soils, 10th edn Macmillan Publishing Co". In: *Inc., New York* (1990).

- [9] Avner Vengosh, Cahit Helvacı, and İsmail H Karamanderesi. "Reply to the comment on "Geochemical constraints for the origin of thermal waters from western Turkey" by Umran Serpen and Tahir Öngür". In: *Applied Geochemistry* 18.7 (2003), pp. 1117–1119.
- [10] Xiaomin Chang et al. "Modelling long-term soil salinity dynamics using Salt-Mod in Hetao Irrigation District, China". In: *Computers and Electronics in Agriculture* 156 (2019), pp. 447–458.
- [11] Girisha Ganjgunte et al. "Organic carbon, nutrient, and salt dynamics in saline soil and switchgrass (*Panicum virgatum* L.) irrigated with treated municipal wastewater". In: *Land degradation & development* 29.1 (2018), pp. 80–90.
- [12] Dennis Wichelns and Manzoor Qadir. "Achieving sustainable irrigation requires effective management of salts, soil salinity, and shallow groundwater". In: *Agricultural Water Management* 157 (2015), pp. 31–38.
- [13] Reeta Kumari et al. "Potential of organic amendments (AM fungi, PGPR, vermicompost and seaweeds) in combating salt stress—a review". In: *Plant Stress* (2022), p. 100111.
- [14] Zied Haj-Amor et al. "Soil salinity and its associated effects on soil microorganisms, greenhouse gas emissions, crop yield, biodiversity and desertification: A review". In: *Science of the Total Environment* 843 (2022), p. 156946.
- [15] Jiangpei Han et al. "Effects of nitrogen fertilization on the acidity and salinity of greenhouse soils". In: *Environmental Science and Pollution Research* 22 (2015), pp. 2976–2986.
- [16] US Salinity Laboratory Staff. "Diagnosis and improvement of saline and alkali soils". In: *Agriculture handbook* 60 (1954), pp. 83–100.

- [17] Rana Munns and Mark Tester. "Mechanisms of salinity tolerance". In: *Annu. Rev. Plant Biol.* 59 (2008), pp. 651–681.
- [18] Edward P Glenn, J Jed Brown, and Eduardo Blumwald. "Salt tolerance and crop potential of halophytes". In: *Critical reviews in plant sciences* 18.2 (1999), pp. 227–255.
- [19] Yoav Yichie et al. "Salinity tolerance in Australian wild *Oryza* species varies widely and matches that observed in *O. sativa*". In: *Rice* 11 (2018), pp. 1–14.
- [20] M Amaranatha Reddy et al. "Breeding for tolerance to stress triggered by salinity in rice". In: *Int. J. Appl. Biol. Pharm. Technol* 5 (2014), pp. 167–176.
- [21] Sulaiman Cheabu et al. "Effects of heat stress at vegetative and reproductive stages on spikelet fertility". In: *Rice Science* 25.4 (2018), pp. 218–226.
- [22] M Djanaguiraman et al. "Rice can acclimate to lethal level of salinity by pre-treatment with sublethal level of salinity through osmotic adjustment". In: *Plant and Soil* 284 (2006), pp. 363–373.
- [23] Glenn B Gregorio. "Tagging salinity tolerance genes in rice using amplified fragment length polymorphism (AFLP)". In: (1997).
- [24] Eugene V Maas and Glenn J Hoffman. "Crop salt tolerance—current assessment". In: *Journal of the irrigation and drainage division* 103.2 (1977), pp. 115–134.
- [25] Ayut Kongpun, Phattana Jaisiri, Benjavan Rerkasem, et al. "Impact of soil salinity on grain yield and aromatic compound in Thai Hom Mali rice cv. Khao Dawk Mali 105". In: *Agriculture and Natural Resources* 54.1 (2020), pp. 74–78.

- [26] Aisha Shereen et al. "Salinity effects on seedling growth and yield components of different inbred rice lines". In: *Pak. J. Bot* 37.1 (2005), pp. 131–139.
- [27] Muhammad Numan et al. "Plant growth promoting bacteria as an alternative strategy for salt tolerance in plants: a review". In: *Microbiological research* 209 (2018), pp. 21–32.
- [28] Kristin Piikki et al. "Perspectives on validation in digital soil mapping of continuous attributes—A review". In: *Soil Use and Management* 37.1 (2021), pp. 7–21.
- [29] Graciela Isabel Metternicht and JA Zinck. "Remote sensing of soil salinity: potentials and constraints". In: *Remote sensing of Environment* 85.1 (2003), pp. 1–20.
- [30] Amal Allbed and Lalit Kumar. "Soil salinity mapping and monitoring in arid and semi-arid regions using remote sensing technology: a review". In: *Advances in remote sensing* 2013 (2013).
- [31] Brian Spies and Peter Woodgate. *Salinity mapping methods in the Australian context*. Department of the Environment and Heritage Canberra, Australia, 2005.
- [32] Taha Gorji, Elif Sertel, and Aysegul Tanik. "Monitoring soil salinity via remote sensing technology under data scarce conditions: A case study from Turkey". In: *Ecological indicators* 74 (2017), pp. 384–391.
- [33] Taha Gorji et al. "Soil salinity analysis of Urmia Lake Basin using Landsat-8 OLI and Sentinel-2A based spectral indices and electrical conductivity measurements". In: *Ecological Indicators* 112 (2020), p. 106173.

- [34] A Azabdaftari and F Sunar. "Soil salinity mapping using multitemporal Landsat data". In: *The International Archives of the Photogrammetry, Remote Sensing and Spatial Information Sciences* 41 (2016), pp. 3–9.
- [35] Abdelgadir Abuelgasim and Rubab Ahammad. "Mapping soil salinity in arid and semi-arid regions using Landsat 8 OLI satellite data". In: *Remote Sensing Applications: Society and Environment* 13 (2019), pp. 415–425.
- [36] Pham Viet Hoa et al. "Soil salinity mapping using SAR sentinel-1 data and advanced machine learning algorithms: A case study at Ben Tre Province of the Mekong River Delta (Vietnam)". In: *Remote Sensing* 11.2 (2019), p. 128.
- [37] Haiyang Shi et al. "A global meta-analysis of soil salinity prediction integrating satellite remote sensing, soil sampling, and machine learning". In: *IEEE Transactions on Geoscience and Remote Sensing* 60 (2021), pp. 1–15.
- [38] Abderrazak Bannari et al. "Sentinel-MSI VNIR and SWIR bands sensitivity analysis for soil salinity discrimination in an arid landscape". In: *Remote Sensing* 10.6 (2018), p. 855.
- [39] Wenzhi Zeng et al. "Predicting near-surface moisture content of saline soils from near-infrared reflectance spectra with a modified Gaussian model". In: *Soil Science Society of America Journal* 80.6 (2016), pp. 1496–1506.
- [40] James L Garrison et al. "Estimation of sea surface roughness effects in microwave radiometric measurements of salinity using reflected global navigation satellite system signals". In: *IEEE Geoscience and Remote Sensing Letters* 8.6 (2011), pp. 1170–1174.
- [41] Simon H Yueh et al. "Error sources and feasibility for microwave remote sensing of ocean surface salinity". In: *IEEE Transactions on Geoscience and Remote Sensing* 39.5 (2001), pp. 1049–1060.

- [42] L Karthikeyan et al. "Four decades of microwave satellite soil moisture observations: Part 1. A review of retrieval algorithms". In: *Advances in Water Resources* 109 (2017), pp. 106–120.
- [43] Xinyang Yu et al. "Precise monitoring of soil salinity in China's Yellow River Delta using UAV-borne multispectral imagery and a soil salinity retrieval index". In: *Sensors* 22.2 (2022), p. 546.
- [44] Ning Yang et al. "Effect of spring irrigation on soil salinity monitoring with UAV-borne multispectral sensor". In: *International Journal of Remote Sensing* 42.23 (2021), pp. 8952–8978.
- [45] Amal Allbed, Lalit Kumar, and Yousef Y Aldakheel. "Assessing soil salinity using soil salinity and vegetation indices derived from IKONOS high-spatial resolution imageries: Applications in a date palm dominated region". In: *Geoderma* 230 (2014), pp. 1–8.
- [46] Ting-Ting Zhang et al. "Using hyperspectral vegetation indices as a proxy to monitor soil salinity". In: *Ecological Indicators* 11.6 (2011), pp. 1552–1562.
- [47] Hong Jiang et al. "Quantitative assessment of soil salinity using multi-source remote sensing data based on the support vector machine and artificial neural network". In: *International journal of remote sensing* 40.1 (2019), pp. 284–306.
- [48] Arastou Zarei, Mahdi Hasanlou, and Masoud Mahdianpari. "A comparison of machine learning models for soil salinity estimation using multi-spectral earth observation data". In: *ISPRS Annals of the Photogrammetry, Remote Sensing and Spatial Information Sciences* 3 (2021), pp. 257–263.

- [49] Cumhuri Aydinalp and Malcolm S Cresser. "The effects of global climate change on agriculture". In: *American-Eurasian Journal of Agricultural & Environmental Sciences* 3.5 (2008), pp. 672–676.
- [50] Robert Mendelsohn. "The impact of climate change on agriculture in developing countries". In: *Journal of Natural Resources Policy Research* 1.1 (2009), pp. 5–19.
- [51] Ali Rahmat and Abdul Mutolib. "Comparison air temperature under global climate change issue in Gifu city and Ogaki city, Japan". In: *Indonesian journal of science and technology* 1.1 (2016), pp. 37–46.
- [52] Sonja Joy Vermeulen et al. "Options for support to agriculture and food security under climate change". In: *Environmental Science & Policy* 15.1 (2012), pp. 136–144.
- [53] Dennis L Corwin. "Climate change impacts on soil salinity in agricultural areas". In: *European Journal of Soil Science* 72.2 (2021), pp. 842–862.
- [54] Taisheng Du et al. "Water use and yield responses of cotton to alternate partial root-zone drip irrigation in the arid area of north-west China". In: *Irrigation Science* 26 (2008), pp. 147–159.
- [55] Nguyen Thi Kim Phuong et al. "Influence of Rice Husk Biochar and Compost Amendments on Salt Contents and Hydraulic Properties of Soil and Rice Yield in Salt-Affected Fields". In: *Agronomy* 10.8 (2020), p. 1101. ISSN: 2073-4395.
- [56] Shabbir A. Shahid, Mohammad Zaman, and Lee Heng. "Soil Salinity: Historical Perspectives and a World Overview of the Problem". In: *Guideline for Salinity Assessment, Mitigation and Adaptation Using Nuclear and Related Techniques*. Cham: Springer International Publishing, 2018, pp. 43–53.

- [57] Wangxia Wang, Basia Vinocur, and Arie Altman. "Plant responses to drought, salinity and extreme temperatures: towards genetic engineering for stress tolerance". In: *Planta* 218.1 (2003), pp. 1–14.
- [58] J. Martinez-Beltran and Clemencia Licon-Manzur. "Overview of salinity problems in the world and FAO strategies to address the problem". In: *Proceedings of the International Salinity Forum* (Jan. 2005), pp. 311–313.
- [59] Pongsak Sahunalu. "Rehabilitation of salt affected lands in Northeast Thailand". In: *Tropics* 13.1 (2003), pp. 39–51.
- [60] Louis S. Gardner. "Report of Investigation - Thailand, Department of Mineral Resources". In: *Thailand Department of Mineral Resources* 11 (1967).
- [61] "Salt and Silt in Ancient Mesopotamian Agriculture". In: *Science* 128.3334 (1958), pp. 1251–1258. ISSN: 00368075, 10959203. (Visited on 06/16/2022).
- [62] Nalun Panpluem et al. "Measuring the Technical Efficiency of Certified Organic Rice Producing Farms in Yasothon Province: Northeast Thailand". In: *Sustainability* 11.24 (2019), p. 6974. ISSN: 2071-1050.
- [63] AUNG NAING Oo, CHULEEMAS BOONTHAI Iwai, and PATCHAREE Sarn-Jan. "Food Security and Socio-economic Impacts of Soil Salinization in Northeast Thailand". In: *International Journal of Environmental and Rural Development* 4.2 (2013), pp. 76–81.
- [64] Koki Homma et al. "Evaluation of Transplanting Date and Nitrogen Fertilizer Rate Adapted by Farmers to Toposequential Variation of Environmental Resources in a Mini-Watershed (Nong) in Northeast Thailand". In: *Plant Production Science* 10.4 (2007), pp. 488–496.
- [65] Roengsak Katawatin and Wilaiwan Kotrapat. "Use of LANDSAT-7 ETM+ with ancillary data for soil salinity mapping in northeast Thailand". In: *Third*

- International Conference on Experimental Mechanics and Third Conference of the Asian Committee on Experimental Mechanics*. Vol. 5852. Society of Photo-Optical Instrumentation Engineers (SPIE) Conference Series. Apr. 2005, pp. 708–716.
- [66] Stephen Grattan et al. "Rice is more sensitive to salinity than previously thought". In: *California agriculture* 56.6 (2002), pp. 189–198.
- [67] Stanley Lutts, JM Kinet, and Jules Bouharmont. "NaCl-induced senescence in leaves of rice (*Oryza sativa*L.) cultivars differing in salinity resistance". In: *Annals of botany* 78.3 (1996), pp. 389–398.
- [68] MF Anshori et al. "Determination of selection criteria for screening of rice genotypes for salinity tolerance." In: *SABRAO Journal of Breeding & Genetics* 50.3 (2018), pp. 279–294.
- [69] D. W. Thorne. "Diagnosis and Improvement of Saline and Alkali Soils". In: *Agronomy Journal* 46.6 (1954), pp. 290–290.
- [70] E. V. Maas and S. R. Grattan. "Crop Yields as Affected by Salinity". In: *Agricultural Drainage*. John Wiley Sons, Ltd, 1999. Chap. 3, pp. 55–108. ISBN: 9780891182306.
- [71] Cathy Clermont-Dauphin et al. "Yield of rice under water and soil salinity risks in farmers' fields in northeast Thailand". In: *Field Crops Research* 118 (2010), pp. 289–296.
- [72] P Wichaidit. "Report on survey and studies of salt-affected soils: Khon Kaen Province". In: *Soil Survey and Classification Section, Land Development Department, Bangkok, Thailand* 20 (1995).
- [73] Koshi Yoshida et al. "Climate change impact on soil salt accumulation in Khon Kaen, Northeast Thailand". In: *Hydrological Research Letters* 15.4 (2021), pp. 92–97.

- [74] Yi Yang et al. "Yearly change in severely salt-damaged areas in paddy fields in Ban Phai in Northeast Thailand". In: *Hydrological Research Letters* 16.1 (2022), pp. 7–11.
- [75] Masayasu Maki et al. "Impact of changes in the relationship between salinity and soil moisture on remote sensing data usage in northeast Thailand". In: *Hydrological Research Letters* 16.2 (2022), pp. 54–58.
- [76] Pichayanun Suwanmontri, Akihiko Kamoshita, and Shu Fukai. "Recent changes in rice production in rainfed lowland and irrigated ecosystems in Thailand". In: *Plant Production Science* 24.1 (2021), pp. 15–28.
- [77] Noppol Arunrat et al. "Soil Organic Carbon in Sandy Paddy Fields of Northeast Thailand: A Review". In: *Agronomy* 10.8 (2020), p. 1061. ISSN: 2073–4395.
- [78] Kewaree Pholkern, Phayom Saraphirom, and Kriengsak Srisuk. "Potential impact of climate change on groundwater resources in the Central Huai Luang Basin, Northeast Thailand". In: *Science of The Total Environment* 633 (2018), pp. 1518–1535. ISSN: 0048-9697.
- [79] K Naklang et al. "Internal efficiency, nutrient uptake, and the relation to field water resources in rainfed lowland rice of northeast Thailand". In: *Plant and soil* 286.1 (2006), pp. 193–208.
- [80] SM Haeefele et al. "Factors affecting rice yield and fertilizer response in rainfed lowlands of northeast Thailand". In: *Field crops research* 98.1 (2006), pp. 39–51.
- [81] Koki Homma et al. "Toposequential variation in soil fertility and rice productivity of rainfed lowland paddy fields in mini-watershed (Nong) in Northeast Thailand". In: *Plant Production Science* 6.2 (2003), pp. 147–153.

- [82] Mainak Ghosh et al. "Optimizing chlorophyll meter (SPAD) reading to allow efficient nitrogen use in rice and wheat under rice-wheat cropping system in eastern India". In: *Plant Production Science* 23.3 (2020), pp. 270–285.
- [83] Xiayang Yu, Pei Xin, and Lu Hong. "Effect of evaporation on soil salinization caused by ocean surge inundation". In: *Journal of Hydrology* 597 (2021), p. 126200. ISSN: 0022-1694.
- [84] Yuting Zhang et al. "Characterization of soil salinization and its driving factors in a typical irrigation area of Northwest China". In: *Science of The Total Environment* 837 (2022), p. 155808.
- [85] CHULEEMAS BOONTHAI Iwai and AJCHARAWADEE Kruapukee. "Using Vermitechnology in Soil Rehabilitation for Rice Production in Salt-affected Area of Northeast Thailand". In: *International Journal of Environmental and Rural Development* 8.2 (2017), pp. 88–93.
- [86] Suriyan Cha-um and Chalernpol Kirdmanee. "Remediation of salt-affected soil by the addition of organic matter: an investigation into improving glutinous rice productivity". In: *Scientia Agricola* 68 (2011), pp. 406–410.
- [87] A Yuvaniyama. "Effect of land use management on groundwater and soil salinization in northeast Thailand". In: *Management of Tropical Sandy Soils for Sustainable Agriculture* (2005), p. 505.
- [88] Phayom Saraphirom, Wanpen Wirojanagud, and Kriengsak Srisuk. "Potential Impact of Climate Change on Area Affected by Waterlogging and Saline Groundwater and Ecohydrology Management in Northeast Thailand." In: *EnvironmentAsia* 6.1 (2013), pp. 19–28.
- [89] Vaclav Smil. *Feeding the world: A challenge for the twenty-first century*. MIT press, 2001.

- [90] NV Nguyen. "Global climate changes and rice food security". In: *Rome: FAO* (2002).
- [91] Liang Wan et al. "Grain yield prediction of rice using multi-temporal UAV-based RGB and multispectral images and model transfer—a case study of small farmlands in the South of China". In: *Agricultural and Forest Meteorology* 291 (2020), p. 108096.
- [92] Yan Guo et al. "Mapping spatial variability of soil salinity in a coastal paddy field based on electromagnetic sensors". In: *PloS one* 10.5 (2015), e0127996.
- [93] Muhammad Nasir Amin et al. "Prediction model for rice husk ash concrete using AI approach: Boosting and bagging algorithms". In: *Structures*. Vol. 50. Elsevier. 2023, pp. 745–757.
- [94] Xiuliang Jin et al. "A review of data assimilation of remote sensing and crop models". In: *European Journal of Agronomy* 92 (2018), pp. 141–152.
- [95] Jinha Jung et al. "The potential of remote sensing and artificial intelligence as tools to improve the resilience of agriculture production systems". In: *Current Opinion in Biotechnology* 70 (2021), pp. 15–22.
- [96] Qi Yang et al. "Deep convolutional neural networks for rice grain yield estimation at the ripening stage using UAV-based remotely sensed images". In: *Field Crops Research* 235 (2019), pp. 142–153.
- [97] Babankumar Bansod et al. "A comparison between satellite based and drone based remote sensing technology to achieve sustainable development: A review". In: *Journal of Agriculture and Environment for International Development (JAEID)* 111.2 (2017), pp. 383–407.

- [98] Yoshio Inoue. "Satellite-and drone-based remote sensing of crops and soils for smart farming—a review". In: *Soil Science and Plant Nutrition* 66.6 (2020), pp. 798–810.
- [99] Mutlu Ozdogan et al. "Remote sensing of irrigated agriculture: Opportunities and challenges". In: *Remote sensing* 2.9 (2010), pp. 2274–2304.
- [100] Jonathan Rigg et al. "More farmers, less farming? Understanding the truncated agrarian transition in Thailand". In: *World Development* 107 (2018), pp. 327–337.
- [101] WanXue Zhu et al. "Estimation of winter wheat yield using optimal vegetation indices from unmanned aerial vehicle remote sensing." In: *Transactions of the Chinese Society of Agricultural Engineering* 34.11 (2018), pp. 78–86.
- [102] Darren Turner, Arko Lucieer, and Christopher Watson. "Development of an Unmanned Aerial Vehicle (UAV) for hyper resolution vineyard mapping based on visible, multispectral, and thermal imagery". In: *Proceedings of 34th International symposium on remote sensing of environment*. 2011, p. 4.
- [103] Syeda Refat Sultana et al. "Normalized difference vegetation index as a tool for wheat yield estimation: a case study from Faisalabad, Pakistan". In: *The Scientific World Journal* 2014 (2014).
- [104] J Marti et al. "Can wheat yield be assessed by early measurements of Normalized Difference Vegetation Index?" In: *Annals of Applied biology* 150.2 (2007), pp. 253–257.
- [105] Shawn C Kefauver et al. "Comparative UAV and field phenotyping to assess yield and nitrogen use efficiency in hybrid and conventional barley". In: *Frontiers in Plant Science* 8 (2017), p. 1733.

- [106] Toshiyuki Takai et al. "Rice yield potential is closely related to crop growth rate during late reproductive period". In: *Field Crops Research* 96.2-3 (2006), pp. 328–335.
- [107] Muhammad Moshiur Rahman, DW Lamb, and JN Stanley. "The impact of solar illumination angle when using active optical sensing of NDVI to infer fAPAR in a pasture canopy". In: *Agricultural and Forest Meteorology* 202 (2015), pp. 39–43.
- [108] DL Harrell et al. "Estimating rice grain yield potential using normalized difference vegetation index". In: *Agronomy Journal* 103.6 (2011), pp. 1717–1723.
- [109] Bo Li et al. "The estimation of crop emergence in potatoes by UAV RGB imagery". In: *Plant Methods* 15.1 (2019), pp. 1–13.
- [110] Meina Zhang et al. "Estimation of maize yield and effects of variable-rate nitrogen application using UAV-based RGB imagery". In: *biosystems engineering* 189 (2020), pp. 24–35.
- [111] John A Hartigan and Manchek A Wong. "Algorithm AS 136: A k-means clustering algorithm". In: *Journal of the royal statistical society. series c (applied statistics)* 28.1 (1979), pp. 100–108.
- [112] Purnima Bholowalia and Arvind Kumar. "EBK-means: A clustering technique based on elbow method and k-means in WSN". In: *International Journal of Computer Applications* 105.9 (2014).
- [113] Huilin Tao et al. "Estimation of crop growth parameters using UAV-based hyperspectral remote sensing data". In: *Sensors* 20.5 (2020), p. 1296.
- [114] Juliane Bendig, Andreas Bolten, and Georg Bareth. "UAV-based imaging for multi-temporal, very high resolution crop surface models to monitor crop

- growth variability". In: *Unmanned aerial vehicles (UAVs) for multi-temporal crop surface modelling* (2013), p. 44.
- [115] Dong-Wook Kim et al. "Modeling and testing of growth status for Chinese cabbage and white radish with UAV-based RGB imagery". In: *Remote Sensing* 10.4 (2018), p. 563.
- [116] Mariana de Jesús Marcial-Pablo et al. "Estimation of vegetation fraction using RGB and multispectral images from UAV". In: *International journal of remote sensing* 40.2 (2019), pp. 420–438.
- [117] Georg Bareth et al. "low-weight and UAV-based hyperspectral full-frame cameras for monitoring crops: spectral comparison with portable spectroradiometer measurements". In: *Unmanned aerial vehicles (UAVs) for multi-temporal crop surface modelling* 103.10.1127 (2015).
- [118] Muhammad Adeel Hassan et al. "A rapid monitoring of NDVI across the wheat growth cycle for grain yield prediction using a multi-spectral UAV platform". In: *Plant science* 282 (2019), pp. 95–103.
- [119] Voon Koo et al. "A new unmanned aerial vehicle synthetic aperture radar for environmental monitoring". In: *Progress In Electromagnetics Research* 122 (2012), pp. 245–268.
- [120] Chuanqi Xie and Ce Yang. "A review on plant high-throughput phenotyping traits using UAV-based sensors". In: *Computers and Electronics in Agriculture* 178 (2020), p. 105731.
- [121] Maitiniyazi Maimaitijiang et al. "Crop monitoring using satellite/UAV data fusion and machine learning". In: *Remote Sensing* 12.9 (2020), p. 1357.

- [122] Antonius GT Schut et al. "Assessing yield and fertilizer response in heterogeneous smallholder fields with UAVs and satellites". In: *Field Crops Research* 221 (2018), pp. 98–107.
- [123] Yi Yang et al. "Rice production in farmer fields in soil salinity classified areas in Khon Kaen, Northeast Thailand". In: *Sustainability* 14.16 (2022), p. 9873.
- [124] Sabine Stuerz et al. "Leaf area development in response to meristem temperature and irrigation system in lowland rice". In: *Field Crops Research* 163 (2014), pp. 74–80.
- [125] L Salazar, F Kogan, and L Roytman. "Use of remote sensing data for estimation of winter wheat yield in the United States". In: *International journal of remote sensing* 28.17 (2007), pp. 3795–3811.
- [126] Alireza Sharifi. "Yield prediction with machine learning algorithms and satellite images". In: *Journal of the Science of Food and Agriculture* 101.3 (2021), pp. 891–896.
- [127] Yolanda M Fernandez-Ordoñez and Jesus Soria-Ruiz. "Maize crop yield estimation with remote sensing and empirical models". In: *2017 IEEE international geoscience and remote sensing symposium (IGARSS)*. IEEE. 2017, pp. 3035–3038.
- [128] Saeed Khaki, Hieu Pham, and Lizhi Wang. "Simultaneous corn and soybean yield prediction from remote sensing data using deep transfer learning". In: *Scientific Reports* 11.1 (2021), p. 11132.
- [129] Fumin Wang et al. "Rice yield estimation based on vegetation index and fluorescence spectral information from UAV hyperspectral remote sensing". In: *Remote Sensing* 13.17 (2021), p. 3390.

- [130] Yan Gong et al. "Remote estimation of rapeseed yield with unmanned aerial vehicle (UAV) imaging and spectral mixture analysis". In: *Plant methods* 14.1 (2018), pp. 1–14.
- [131] D Casanova, GF Epema, and J1 Goudriaan. "Monitoring rice reflectance at field level for estimating biomass and LAI". In: *Field Crops Research* 55.1-2 (1998), pp. 83–92.
- [132] Fei Li et al. "Evaluating hyperspectral vegetation indices for estimating nitrogen concentration of winter wheat at different growth stages". In: *Precision Agriculture* 11 (2010), pp. 335–357.
- [133] AR Huete et al. "A comparison of vegetation indices over a global set of TM images for EOS-MODIS". In: *Remote sensing of environment* 59.3 (1997), pp. 440–451.
- [134] Eugene V Maas and SR Grattan. "Crop yields as affected by salinity". In: *Agricultural drainage* 38 (1999), pp. 55–108.
- [135] Kirsten Butcher et al. "Soil salinity: A threat to global food security". In: *Agronomy Journal* 108.6 (2016), pp. 2189–2200.
- [136] P Thaikla et al. "Land degradation and amendment". In: *Land Development Department, Bangkok, Thailand* 14 (2010).
- [137] Louis S Gardner. "Salt resources of Thailand". In: *Report of Investigation-Thailand, Department of Mineral Resources* 11 (1967).
- [138] Uma Seeboonruang. "Relationship between groundwater properties and soil salinity at the Lower Nam Kam River Basin in Thailand". In: *Environmental Earth Sciences* 69.6 (2013), pp. 1803–1812.

- [139] Koshi Yoshida et al. "Climate change impact on soil salt accumulation in Khon Kaen, Northeast Thailand". In: *Hydrological Research Letters* 15.4 (2021), pp. 92–97.
- [140] S Ratanopad and W Kainz. "Using GIS and map data for the analysis of the expansion of salinized soils". In: *ISPRS Commission IV symposium on Geospatial databases for sustainable development*. 2006.
- [141] Koki Homma et al. "Evaluation of transplanting date and nitrogen fertilizer rate adapted by farmers to toposequential variation of environmental resources in a mini-watershed (Nong) in northeast Thailand". In: *Plant production science* 10.4 (2007), pp. 488–496.
- [142] Sukanya Sujariya et al. "Rainfall variability and its effects on growing period and grain yield for rainfed lowland rice under transplanting system in Northeast Thailand". In: *Plant Production Science* 23.1 (2020), pp. 48–59.
- [143] Jitarree Saisema and Adcharaporn Pagdee. "Ecological and socioeconomic factors that affect rice production in saline soils, Borabue, Mahasarakham, Thailand: Implications for farm management practices". In: *Agroecology and Sustainable Food Systems* 39.1 (2015), pp. 62–82.
- [144] AUNG NAING Oo, CHULEEMAS BOONTHAI Iwai, and PATCHAREE Saenjan. "Food security and socio-economic impacts of soil salinization in northeast Thailand". In: *Environ. Rural Dev* 4 (2013), pp. 76–81.
- [145] Korachan Thanasilungura et al. "Improvement of a RD6 rice variety for blast resistance and salt tolerance through marker-assisted backcrossing". In: *Agronomy* 10.8 (2020), p. 1118.
- [146] Masayasu Maki et al. "Evaluation of the relationship between electric conductivity and spectral index for soil salinity mapping of rice paddy field in

- Khon Kaen Province". In: *THA 2019 International Conference TC318-1*. 2019, pp. 1–4.
- [147] Fabian Pedregosa et al. "Scikit-Learn: Machine Learning in Python". In: *J. Mach. Learn. Res.* 12.null (Nov. 2011), pp. 2825–2830. ISSN: 1532-4435.
- [148] Olivier Chapelle, Patrick Haffner, and Vladimir N Vapnik. "Support vector machines for histogram-based image classification". In: *IEEE transactions on Neural Networks* 10.5 (1999), pp. 1055–1064.
- [149] Vladimir Vapnik and Rauf Izmailov. "Knowledge transfer in SVM and neural networks". In: *Annals of Mathematics and Artificial Intelligence* 81.1-2 (2017), pp. 3–19.
- [150] Fred K Hoehler. "Bias and prevalence effects on kappa viewed in terms of sensitivity and specificity". In: *Journal of clinical epidemiology* 53.5 (2000), pp. 499–503.
- [151] Fausto Guzzetti et al. "Estimating the quality of landslide susceptibility models". In: *Geomorphology* 81.1-2 (2006), pp. 166–184.
- [152] J Richard Landis and Gary G Koch. "An application of hierarchical kappa-type statistics in the assessment of majority agreement among multiple observers". In: *Biometrics* (1977), pp. 363–374.
- [153] Rajendra Shrestha. "Relating soil electrical conductivity to remote sensing and other soil properties for assessing soil salinity in northeast Thailand". In: *Land Degradation Development* 17 (Nov. 2006), pp. 677–689.
- [154] Nguyen, Tetsuhiro Watanabe, and Funakawa. "Spatiotemporal variability in soil salinity and its effects on rice (*Oryza sativa* L.) production in the north central coastal region of Vietnam". In: *Soil Science and Plant Nutrition* 60 (Nov. 2014).

- [155] Terdsak Subhasaram Kenzo Miura. "Soil Salinity after Deforestation and Control by Reforestation in Northeast Thailand". In: *Japan International Research Center for Agricultural Sciences* 24 (1990), pp. 186–196.
- [156] Pongsak Sahunalu. "Rehabilitation of salt affected lands in Northeast Thailand". In: *Tropics* 13.1 (2003), pp. 39–51.
- [157] Rui Manuel Almeida Machado and Ricardo Paulo Serralheiro. "Soil salinity: effect on vegetable crop growth. Management practices to prevent and mitigate soil salinization". In: *Horticulturae* 3.2 (2017), p. 30.
- [158] Kewaree Pholkern, Phayom Saraphirom, and Kriengsak Srisuk. "Potential impact of climate change on groundwater resources in the Central Huai Luang Basin, Northeast Thailand". In: *Science of the Total Environment* 633 (2018), pp. 1518–1535.
- [159] C Mongkolsawat and S Paiboonsak. "GIS application to spatial distribution of soil salinity potential in northeast Thailand". In: *Proceedings of the 27th Asian Conference on Remote Sensing of Mongolia*. 2006, pp. 1–5.
- [160] Somsri ARUNIN and Pirach PONGWICHIAN. "Salt-affected soils and management in Thailand". In: *Bulletin of the Society of Sea Water Science, Japan* 69.5 (2015), pp. 319–325.
- [161] Boonrat Jongdee. "Designing a national breeding program for developing drought-tolerant rainfed lowland varieties: the Thailand experience". In: *Breeding rice for drought-prone environments* (2003), p. 64.
- [162] Anan Polthanee, Arunee Promkhumbut, and Jiraporn Bamrungrai. "Drought impact on rice production and farmers' adaptation strategies in Northeast Thailand". In: *International Journal of Environmental and Rural Development* 5.1 (2014), pp. 45–52.

- [163] C Clermont-Dauphin et al. "Yield of rice under water and soil salinity risks in farmers' fields in northeast Thailand". In: *Field Crops Research* 118.3 (2010), pp. 289–296.
- [164] SM Haefele et al. "Factors affecting rice yield and fertilizer response in rain-fed lowlands of northeast Thailand". In: *Field crops research* 98.1 (2006), pp. 39–51.